The Plant Cell, Vol. 25: 4166–4182, October 2013, www.plantcell.org

A Rice *cis*-Natural Antisense RNA Acts as a Translational Enhancer for Its Cognate mRNA and Contributes to Phosphate Homeostasis and Plant Fitness[C][W]

Mehdi Jabnoune,[a] David Secco,[a,1] Cécile Lecampion,[b] Christophe Robaglia,[b] Qingyao Shu,[c] and Yves Poirier[a,2]

[a] Department of Plant Molecular Biology, University of Lausanne, Lausanne CH-1015, Switzerland

[b] Laboratory of Plant Genetics and Biophysics, Centre National de la Recherche Scientifique, Unité Mixte de Recherche 7265, Commissariat à l'Energie Atomique, Institute of Environmental Biology and Biotechnology, Aix Marseille University, Faculty of Sciences, Luminy, Marseille F-13009, France

[c] Institute of Nuclear Agricultural Sciences, Zhejiang University, Hangzhou 310029, China

ORCID ID: 0000-0002-9562-1226 (M.J.).

cis*-natural antisense transcripts (*cis*-NATs) are widespread in plants and are often associated with downregulation of their associated sense genes. We found that a *cis*-NAT positively regulates the level of a protein critical for phosphate homeostasis in rice (*Oryza sativa*). *PHOSPHATE1;2* (*PHO1;2*), a gene involved in phosphate loading into the xylem in rice, and its associated *cis*-NAT$_{PHO1;2}$ are both controlled by promoters active in the vascular cylinder of roots and leaves. While the *PHO1;2* promoter is unresponsive to the plant phosphate status, the *cis*-NAT$_{PHO1;2}$ promoter is strongly upregulated under phosphate deficiency. Expression of both *cis*-NAT$_{PHO1;2}$ and the PHO1;2 protein increased in phosphate-deficient plants, while the *PHO1;2* mRNA level remained stable. Downregulation of *cis*-NAT$_{PHO1;2}$ expression by RNA interference resulted in a decrease in PHO1;2 protein, impaired the transfer of phosphate from root to shoot, and decreased seed yield. Constitutive overexpression of NAT$_{PHO1;2}$ in *trans* led to a strong increase of PHO1;2, even under phosphate-sufficient conditions. Under all conditions, no changes occurred in the level of expression, sequence, or nuclear export of *PHO1;2* mRNA. However, expression of *cis*-NAT$_{PHO1;2}$ was associated with a shift of both *PHO1;2* and *cis*-NAT$_{PHO1;2}$ toward the polysomes. These findings reveal an unexpected role for *cis*-NAT$_{PHO1;2}$ in promoting *PHO1;2* translation and affecting phosphate homeostasis and plant fitness.

INTRODUCTION

Recent studies of eukaryotic genomes using experimental approaches, such as deep RNA sequencing and tiling microarrays, have revealed that a large part of the genome of plants, fungi, and metazoans is transcribed and that noncoding regulatory RNAs (ncRNAs) play key roles in modulating gene expression. One group of such RNAs encompasses the small ncRNAs generated via processing from longer precursors and includes microRNAs (miRNAs) and short interfering RNAs (siRNAs). These small ncRNAs have well established roles in various gene silencing mechanisms involving the regulation of DNA methylation, mRNA processing, or translation (Ghildiyal and Zamore, 2009; Chen, 2010).

Long ncRNAs are typically >200 nucleotides in length and are generated without extensive processing except for splicing, capping, and polyadenylation. Natural antisense transcripts (NATs) represent one class of long RNAs containing sequences that are complementary to sense mRNAs (Lavorgna et al., 2004; Lapidot and Pilpel, 2006). While some NATs are known to encode proteins, the majority of NATs in eukaryote genomes are thought to be noncoding. NATs can be grouped into two categories, *cis*-NATs and *trans*-NATs. *cis*-NAT pairs are transcribed from opposing DNA strands at the same genomic locus and have a variety of orientations and differing lengths of overlap between the regions having perfect sequence complementarity, whereas *trans*-NAT pairs are transcribed from different loci and form partial complementarity to the sense transcript (Lapidot and Pilpel, 2006; Wang et al., 2006; Li et al., 2008).

Genome-wide analyses of numerous organisms, including human, mouse, *Drosophila melanogaster*, *Arabidopsis thaliana*, and rice (*Oryza sativa*) have revealed the widespread existence of NATs in eukaryotes, with ~10 to 30% of mRNA-encoding genes having an associated NAT (Misra et al., 2002; Kiyosawa et al., 2003; Osato et al., 2003; Yelin et al., 2003; Katayama et al., 2005; Wang et al., 2005; Li et al., 2006; Zhang et al., 2006). Studies performed mainly in yeast and animals have revealed that NATs can participate in a broad range of regulatory events, including transcriptional interference, RNA masking-induced alternative splicing, X chromosome inactivation, genomic imprinting, RNA editing, DNA methylation, and siRNA-induced gene silencing (Faghihi and Wahlestedt, 2009; Au et al., 2011; Rinn and Chang, 2012). While the expression of some NATs has been associated with transcriptional activation, NAT expression primarily results in the suppression of gene expression and involves pathways

[1] Current address: Australian Research Council Centre of Excellence in Plant Energy Biology, University of Western Australia, Crawley WA 6009, Australia.

[2] Address correspondence to yves.poirier@unil.ch.

The author responsible for distribution of materials integral to the findings presented in this article in accordance with the policy described in the Instructions for Authors (www.plantcell.org) is: Yves Poirier (yves.poirier@unil.ch).

[C] Some figures in this article are displayed in color online but in black and white in the print edition.

[W] Online version contains Web-only data.

www.plantcell.org/cgi/doi/10.1105/tpc.113.116251

leading to transcriptional downregulation, such as histone modification and the recruitment of chromatin modifiers, or posttranscriptional downregulation, such as the generation of siRNAs (Ponting et al., 2009).

In plants, despite the large number of NATs predicted or identified in *Arabidopsis* and rice, our current knowledge of their role in gene expression is limited to a few loci that are mainly involved in developmental control or adaptive responses to changing environmental conditions. All documented effects of NAT expression in plants have so far been associated with downregulation of gene expression. For example, the control of flowering in *Arabidopsis* by cold treatment was shown to involve expression of *cis*-NATs associated with the *FLOWERING LOCUS C* (*FLC*) locus, leading to *FLC* silencing via chromatin modification (Swiezewski et al., 2007, 2009; Liu et al., 2010). Expression of a noncoding *cis*-NAT associated with a cellulose synthase gene in barley (*Hordeum vulgare*) or a gene modulating plant immunity against a bacterial pathogen in *Arabidopsis* has been shown to trigger siRNA synthesis and lead to a downregulation of their respective target gene (Katiyar-Agarwal et al., 2006; Held et al., 2008). A similar mechanism involving the generation of siRNA and target downregulation was shown in two cases of convergent protein-coding genes overlapping in their 3′ end and involving male gametophyte function and plant response to salt stress (Borsani et al., 2005; Ron et al., 2010). The involvement of a *cis*-NAT in regulating the activity of the *SHOOTING* gene responsible for cytokinin synthesis has also been suggested to occur via degradation of *Sho* double-stranded RNA (Zubko and Meyer, 2007).

Here, we find a role for a *cis*-NAT in the homeostasis of Pi, one of the main nutrients limiting plant growth in most environments. Plants have evolved elaborate mechanisms to sense and adapt to low Pi. For example, microarray studies have revealed that several hundred genes are either induced or repressed following Pi starvation (Misson et al., 2005; Morcuende et al., 2007; Müller et al., 2007). Some of the important genes that are regulated by Pi deficiency are involved in the uptake of Pi from the environment and its controlled transport throughout the plant, such as members of the *PHOSPHATE TRANSPORTER* gene family, which encode H^+−Pi cotransporters (Misson et al., 2005; Morcuende et al., 2007; Müller et al., 2007; Woo et al., 2012). *Arabidopsis PHO1* is primarily expressed in root vascular tissues and is involved in the export of Pi to the apoplastic space of xylem vessels (Hamburger et al., 2002; Stefanovic et al., 2011; Arpat et al., 2012). The *Arabidopsis pho1* null mutant shows a strong reduction of Pi loading into the xylem and displays a typical Pi-deficient phenotype in aerial parts of the plant, resulting in an overall reduction in shoot growth and seed yield (Hamburger et al., 2002). The expression of *Arabidopsis PHO1* and the steady state level of PHO1 are increased under Pi deficiency (Stefanovic et al., 2007).

The rice genome contains three homologs of *PHO1*, and mutant analysis revealed that Os-*PHO1;2* was the functional ortholog of At-*PHO1*, being the main gene responsible for the loading of Pi into the xylem vessel in rice (Secco et al., 2010). An interesting feature distinguishing the three rice *PHO1* genes from their *Arabidopsis* homologs is the presence of *cis*-NATs associated with all of them (Secco et al., 2010). These *cis*-NATs overlap with the 5′ coding exons of the genes. Analysis of the expression profiles of the sense and *cis*-NAT pairs of the rice PHO1 genes revealed distinct patterns of expression in response to Pi deficiency. In particular, while the Os-*PHO1;2* transcript level remained stable under Pi deficiency, its associated *cis*-$NAT_{PHO1;2}$ was strongly and specifically upregulated under the same nutrient deficiency (Secco et al., 2010). This expression pattern led us to investigate a potential role for *cis*-$NAT_{PHO1;2}$ in regulating PHO1;2 expression and to study its consequences on Pi homeostasis in rice.

RESULTS

Expression Pattern of *PHO1;2* and Its Associated *cis*-$NAT_{PHO1;2}$

To examine the relationship between the expression pattern of *PHO1;2* and its associated *cis*-$NAT_{PHO1;2}$, we generated transgenic rice lines expressing the β-glucuronidase (GUS) reporter under the control of the promoter sequence of the Os-*PHO1;2* sense gene ($Pro_{OsPHO1;2\text{-}S}$:GUS) or the *cis*-$NAT_{PHO1;2}$ ($Pro_{cis\text{-}NAT}$:GUS) (Figure 1A). For each construct, 10 independent transgenic lines were examined by GUS staining. Four representative lines for each construct were selected for detailed analysis (Figure 1; see Supplemental Figure 1 online). Transgenic plants used for staining were cultured for 30 d in nutrient solution containing 1 mM Pi (+Pi treatment) or for 7 d on Pi-sufficient medium and then transferred to Pi-deficient medium for 23 d (−Pi treatment). Plants grown in medium without Pi were effectively starved for the nutrient, as determined by the low shoot Pi content and the induction of *INDUCED BY PHOSPHATE STARVATION1* (*IPS1*), a gene known to be strongly upregulated by Pi deficiency (Hou et al., 2005) (see Supplemental Figure 2 online). $Pro_{OsPHO1;2\text{-}S}$:GUS lines grown in Pi-deficient medium had GUS signal in the stele of the crown root (Figure 1B), as well as in the primary and lateral roots (see Supplemental Figure 3A online). Root tips containing meristematic tissues showed no GUS expression (see Supplemental Figure 3C online). Sections of roots revealed GUS staining primarily in the xylem parenchyma cells (Figure 1C). In shoots, GUS staining occurred in the large and small vascular bundles (Figure 1D). Cross sections of GUS-stained leaf blades showed high expression in vascular tissues, including xylem parenchyma, phloem sieve elements, and companion cells (Figure 1E). No GUS staining was detectable in floral structures. The same pattern of GUS expression in the different tissues was found in $Pro_{OsPHO1;2\text{-}S}$:GUS lines grown in Pi-sufficient medium, with only a slight decrease in GUS activity relative to plants grown in Pi-deficient medium (Figure 1F).

Analysis of the $Pro_{cis\text{-}NAT}$:GUS transgenic lines showed no GUS staining in shoots, roots, or floral structures for plants grown in medium with Pi. In sharp contrast, strong GUS staining was observed for plants grown in medium without Pi. For leaves and roots, the pattern of GUS expression was identical to the $Pro_{OsPHO1;2\text{-}S}$:GUS lines, with strong staining in the large and small vascular bundles of shoots and the stele of the crown root (Figures 1G to 1J) and primary and lateral roots (see Supplemental Figure 3B online), but not in the root tip (see Supplemental Figure 3D online). In flowers, GUS staining was observed in pollen and the vascular cylinder of the anther (see Supplemental Figure 4 online). For plants grown under Pi-deficient conditions, GUS activity observed in roots and leaves of $Pro_{cis\text{-}NAT}$:GUS lines was ~5.5- and 7.8-fold higher, respectively, than for $Pro_{OsPHO1;2\text{-}S}$:GUS lines (Figure 1F). These

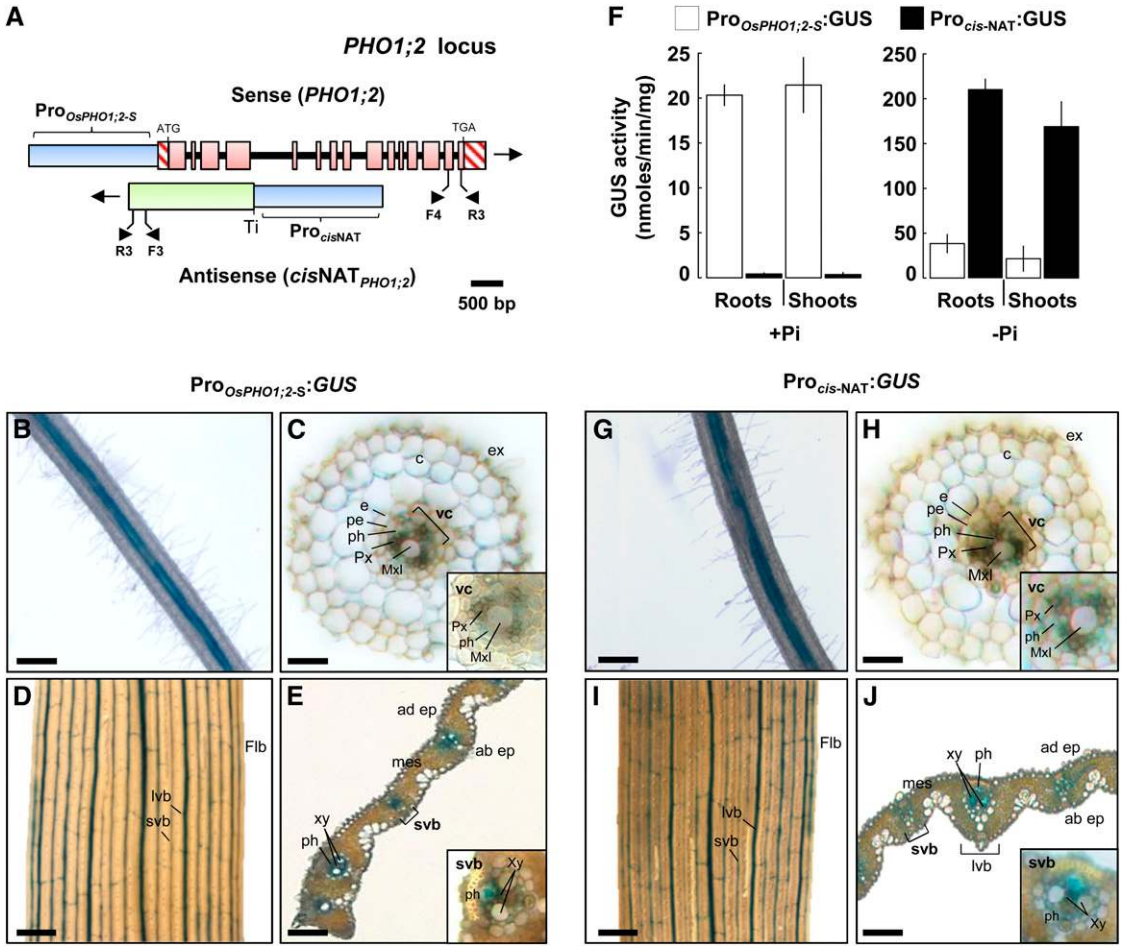

Figure 1. Expression Pattern and Quantification of GUS Activity in Pro$_{OsPHO1;2\text{-}S}$:GUS and Pro$_{cis\text{-}NAT}$:GUS Transgenic Lines.

(A) Schematic showing the genomic organization of the *PHO1;2* locus. The 2-kb promoter regions of *PHO1;2* and *cis*-NAT$_{PHO1;2}$ used to direct the expression of the GUS reporter gene are indicated by blue boxes. Exons are indicated by open red boxes, 3′ and 5′ UTRs by red hatched boxes, and introns as black lines. The DNA region giving rise to the *cis*-NAT$_{PHO1;2}$ transcript is indicated by the green box. Small arrows indicate the location of the primers used for strand-specific quantitative RT-PCR.

(B) to **(E)** and **(G)** to **(J)** Representative staining of GUS activity in 30-d-old Pi-deficient plants expressing Pro$_{OsPHO1;2\text{-}S}$:GUS (**[B]** to **[E]**) or Pro$_{cis\text{-}NAT}$:GUS (**[G]** to **[J]**). ab ep, abaxial epidermis; ad ep, adaxial epidermis; c, cortex; e, endodermis; ex, exodermis; lvb, large vascular bundle; mes, mesophyll; MxI, metaxylem I; pe, pericycle; ph, phloem; Px, protoxylem; svb, small vascular bundle; vc, vascular cylinder; xy, xylem. Bars = 500 μm in **(B)** and **(G)**, 100 μm in **(C)**, **(E)**, **(H)**, and **(J)**, and 1 mm in **(D)** and **(I)**.

(B) and **(G)** Intact crown root.

(C) and **(H)** Cross section of the primary root 2 cm from the tip and magnification (inset) of the central region of the vascular cylinder.

(D) and **(I)** Flag leaf blade.

(E) and **(J)** Cross section of the flag leaf blade and magnification of the small vascular bundle region.

(F) Fluorometric quantification of GUS activity in Pro$_{OsPHO1;2\text{-}S}$:GUS and Pro$_{cis\text{-}NAT}$:GUS transgenic lines under Pi-sufficient (+Pi) or Pi-deficient (−Pi) conditions. GUS activity was measured using crude extracts. Five transgenic plants from lines transformed with each construct were employed for GUS quantification. Data are mean ± SE of GUS activity from three independent experiments.

results revealed that the activities of the promoters of both *PHO1;2* and its associated *cis*-NAT$_{PHO1;2}$ largely overlapped, driving gene expression in cells of the vascular cylinder in both shoots and roots.

No Detectable Expression of Proteins from Open Reading Frames Present in *cis*-NAT$_{PHO1;2}$

The *cis*-NAT$_{PHO1;2}$ transcript was analyzed for the presence of open reading frames (ORFs) that could encode polypeptides composed of at least 40 amino acids. Three such ORFs were found, with ORF1, ORF2, and ORF3 potentially encoding polypeptides of 160, 136, and 103 amino acids in length, respectively (Figure 2A). ORF2 is enclosed within the sequence of ORF1 but uses a different reading frame. Analysis of the ORF sequences by BLAST did not reveal any proteins with significant similarity to ORF1 and ORF3. For ORF2, the only similarity found was a putative polypeptide encoded by a *cis*-NAT associated

with a *PHO1* homolog in maize (*Zea mays*) (LOC100278095) (see Supplemental Figure 5 online). The region harboring the ORF in the maize *cis*-NAT overlaps with the third exon of maize *PHO1* (see Supplemental Figure 5 online). Since the third base of each codon of the rice *cis*-NAT$_{PHO1;2}$ ORF2 and of the maize *cis*-NAT ORF aligns with the third base for codons of their respective PHO1 protein, the apparent conservation in the ORFs of the maize and rice *cis*-NATs simply could be due to the high similarity between the rice and maize PHO1 proteins in this region.

To determine if proteins were produced from any of these ORFs in plants, transgenic lines were created that overexpressed a modified NAT$_{PHO1;2}$ by adding a distinct epitope tag (HA, MYC, or FLAG) at the 3′ end of each of the three ORFs (Figure 2A). Although the addition of an HA tag to ORF2 modifies the sequence of ORF1 by adding 10 codons before the terminal FLAG epitope, such a modification of the 3′ end of ORF1 would be unlikely to affect its translation potential into protein. The modified NAT$_{PHO1;2}$ was under the control of the constitutive 2x cauliflower mosaic virus 35S promoter and transformed in rice. Quantitative RT-PCR analysis revealed that the transgene was strongly expressed in several independent lines, reaching a 10-fold higher level compared with the expression of the endogenous *cis*-NAT$_{PHO1;2}$ in shoots (Figure 2B). Analysis by immunoblot of the shoot protein extracts from these transgenic lines using antibodies recognizing each of the three epitopes failed to detect any polypeptide of the expected size, while the recombinant proteins expressed in bacteria were readily detected (Figure 2C). The detection limit of the immunoblot assay

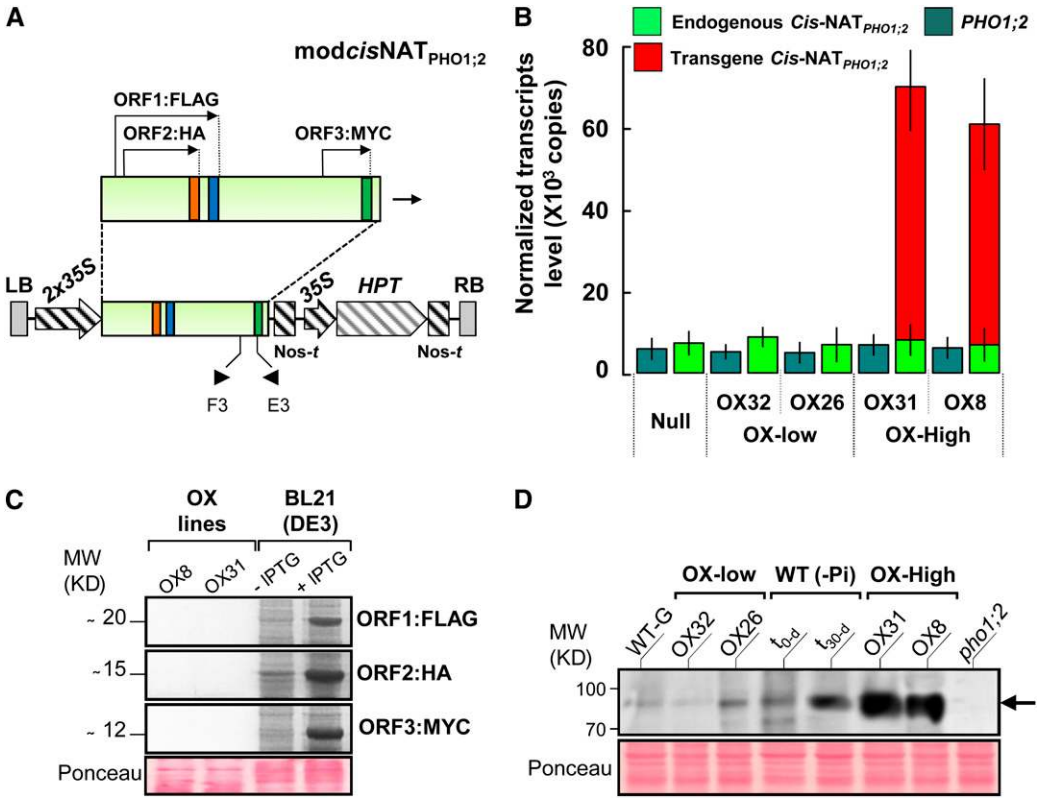

Figure 2. Expression of an Epitope-Tagged *cis*-NAT$_{PHO1;2}$ Construct.

(A) Schematic of the modified *cis*-NAT$_{PHO1;2}$ cDNA (mod*cis*-NAT$_{PHO1;2}$) used to generate overexpressing lines containing epitope-tagged ORFs (top panel) and the overexpression cassette in the construct pMDC32-mod*cis*NAT$_{PHO1;2}$ (bottom panel). The synthetic fragment was generated by adding distinct epitope tags (FLAG, HA, and MYC) at the 3′ end of each of the three longest ORFs. Transcription is derived from the double cauliflower mosaic virus (2×35S) promoter. LB, left T-DNA border; NOS-t, nopaline synthase terminator; HPT, hygromycin phosphotransferase; RB, right T-DNA border. Small arrowheads indicate position of primers F3 and E3 used to detect the expression of the transgene.

(B) Quantitative RT-PCR analysis of *cis*-NAT$_{PHO1;2}$ (endogenous and transgenic mod*cis*-NAT$_{PHO1;2}$) and *PHO1;2* expression level. RNA was extracted from the shoots of OX transgenic lines showing high (OX31 and OX8) or no detectable (OX32 and OX26) expression of the transgenic mod*cis*-NAT$_{PHO1;2}$ transcript. Transgenic lines and the corresponding null segregants are 4-week-old plants grown in Pi-sufficient conditions. Data are means ± SE (n = 4)

(C) Immunoblot analysis on shoot protein extract of two overexpressing lines (OX8 and OX31) using antibodies against the epitope tags. As controls, the fusions ORF1:FLAG, ORF2:HA, and ORF3:Myc were independently expressed in the bacterial strain BL21 (DE3) using a vector inducible by β-D-1-thiogalactopyranoside. MW, molecular mass.

(D) Immunoblot analysis of PHO1;2 in the shoots of mod*cis*NAT$_{PHO1;2}$-OX lines. Wild-type plants grown in the greenhouse (WT-G) and the *pho1;2* null mutant were used as controls. The induction of PHO1;2 synthesis in wild-type plants after 0 d ($t_{0\text{-}d}$) and 30 d ($t_{30\text{-}d}$) of Pi starvation is also shown. The position of PHO1;2 is indicated by the black arrow.

was estimated at 0.3 ng of epitope tag polypeptide per microgram of total protein for ORF1 and ORF2 and 1.5 ng of epitope tag polypeptide per microgram of total protein for OFR3. Thus, there was no evidence for significant expression of polypeptides from the *cis*-NAT$_{PHO1;2}$, indicating that the transcript was likely to be noncoding.

Correlation between *cis*-NAT$_{PHO1;2}$ Expression and PHO1;2 Protein Level

The relationship between the expression of *PHO1;2* and its associated *cis*-NAT$_{PHO1;2}$ with the synthesis of PHO1;2 protein was analyzed in shoots and roots of plants grown in Pi-deficient medium. Rice seedlings grown for 14 d in Pi-sufficient medium were transferred to Pi-deficient medium for 5 to 30 d, and one set of plants was switched back to Pi-sufficient medium for 24 h at 30 d (R+1, where R represents recovery). Immunoblot analysis was performed using microsomal extracts from roots and shoots and polyclonal antibodies against PHO1;2 (see Supplemental Figure 6 online). In plants grown under Pi-sufficient media for 14 d (day 0), PHO1;2 was weakly expressed in both roots and shoots, but the protein level started to increase 15 to 20 d after transfer to Pi-deficient medium and reached a maximum at 30 d (Figures 3A and 3B). Upon a 24-h resupply of Pi to 30-d-old Pi-deficient plants, the amount of PHO1;2 strongly decreased, reaching levels similar to Pi-sufficient plants (Figures 3A and 3B) and revealing that the steady state level of PHO1;2 was directly affected by the Pi supply.

Analysis of the expression of *PHO1;2* and *cis*-NAT$_{PHO1;2}$ was performed by quantitative RT-PCR using a subset of the same plants used for protein analysis (Figures 3C and 3D). In Pi-sufficient conditions (0 d), *PHO1;2* and *cis*-NAT$_{PHO1;2}$ were both expressed in roots at a level 3.5-fold higher than in shoots. After 15 and 30 d of growth in Pi-deficient medium, the sense transcript levels remained at a fairly constant level, while the *cis*-NAT$_{PHO1;2}$ transcript levels increased gradually, for both roots and shoots. In the last day of Pi starvation, *cis*-NAT$_{PHO1;2}$ transcripts were increased by 4 times in the roots and 8 times in the shoots compared with 0 d. Upon a 1-d Pi resupply, *cis*-NAT$_{PHO1;2}$ expression decreased strongly in both roots and shoots, reaching levels slightly below those of Pi-sufficient plants. The kinetics of changes in *PHO1;2* and *cis*-NAT$_{PHO1;2}$ expression resulted in a strong shift in the ratios of antisense to sense transcripts, with a ratio of ~1 for roots and shoots of Pi-sufficient plants, and a ratio of 9 in shoots and 4.5 in roots after 30 d of Pi starvation. Overall, these results show that the steady state level of PHO1;2 protein followed the same abundance profile as the antisense transcript, revealing a positive relationship between *cis*-NAT$_{PHO1;2}$ transcript expression and PHO1;2 accumulation.

Downregulation of *cis*-NAT$_{PHO1;2}$ Expression Reduced PHO1;2 Levels via a Posttranscriptional Mechanism

To better understand the relationship between *cis*-NAT$_{PHO1;2}$ expression and the synthesis of PHO1;2 protein, we generated transgenic plants in which *cis*-NAT$_{PHO1;2}$ expression was downregulated by RNA interference (RNAi) using a chimeric 447-bp target sequence that was complementary to the *cis*-NAT$_{PHO1;2}$ transcript (which is an intronless transcript) but not to the exons of the spliced sense *PHO1;2* transcript (Figure 4A). The hairpin RNAi construct contained two inverted repeats of the target sequence linked by a 920-bp fragment of the *Escherichia coli uidA* gene, and the whole cassette was under the control of the maize *ubiquitin1* promoter, which has been shown to drive high expression of foreign genes in transgenic rice (Figure 4A) (Uchimiya et al., 1993).

Sixteen independent transgenic lines were examined by PCR for the presence of the T-DNA vector (*HPT* gene) and the RNAi cassette (GUS linker) and by RT-PCR for expression of the RNAi cassette (GUS linker) and its effectiveness in downregulating *cis*-NAT$_{PHO1;2}$ expression (see Supplemental Figure 7 online). *cis*-NAT$_{PHO1;2}$ expression was reduced in 14 independent RNAi lines that had inherited the transgene, and two of these lines (named Ri1 and Ri2) were selected for further analysis. RNA was isolated from shoots and roots of plants grown for 7 d on Pi-sufficient medium and then transferred to either Pi-deficient (−Pi) or Pi-sufficient (+Pi) medium for 21 d. Quantitative RT-PCR confirmed that the *cis*-NAT$_{PHO1;2}$ transcript level was strongly decreased in lines Ri1 and Ri2 in comparison to that in wild-type plants in both roots (Figure 4B) and shoots (Figure 4C) of plants grown in Pi-sufficient or Pi-deficient media. By contrast, the level of the sense *PHO1;2* transcript was similar between wild-type control and transgenic RNAi lines in both Pi treatments (Figures 4B and 4C). Expression of the RNAi cassette thus led to a reversal in the antisense to sense transcript ratio, which became ~0.05 in roots and 0.2 in shoots.

Next, the effect of a reduction of *cis*-NAT$_{PHO1;2}$ expression on the synthesis of PHO1;2 protein was analyzed. For this purpose, we compared the protein level of wild-type plants to the RNAi transgenic lines in both roots and shoots. Two-week-old rice seedlings were subjected to Pi starvation for 15 and 30 d, and one set of plants was switched back to Pi-sufficient medium for 24 h at 30 d (R+1). Microsomal proteins were extracted at days 0, 15, and 30 and R+1 from roots and shoots and analyzed by immunoblot with antibodies against PHO1;2. While PHO1;2 protein was clearly detected in roots and shoots of wild-type plants grown for 30 d in Pi-sufficient medium, no signal was detectable in the roots or shoots of the two RNAi lines, irrespective of Pi treatment (Figures 4D and 4E).

To ensure that the sense *PHO1;2* transcript detected by quantitative RT-PCR was not cleaved by the RNAi targeting the *cis*-NAT$_{PHO1;2}$, we conducted an RNase protection assay (RPA) to detect full-length transcripts. ^{32}P-labeled full-length single-stranded RNA probe was used to detect both the sense *PHO1;2* RNA and *cis*-NAT$_{PHO1;2}$. RNA samples were prepared from wild-type plants grown either on −Pi or +Pi medium and also from RNAi lines grown on −Pi medium. Using the probe detecting the *PHO1;2* sense mRNA, a single RNase protected fragment of 2386 nucleotides was detected in both roots and shoots in the RNAi lines and in the wild type (Figure 4F), in agreement with the expression of a full-length mRNA. The signal strength obtained between wild-type and RNAi samples was similar, supporting the conclusion that the level of expression of the *PHO1;2* sense mRNA was not influenced either by Pi nutritional status or expression of the RNAi directed toward the *cis*-NAT$_{PHO1;2}$.

RPA analysis using a single-strand probe against *cis*-NAT$_{PHO1;2}$ revealed a single band of 1652 nucleotides in wild-type plants in

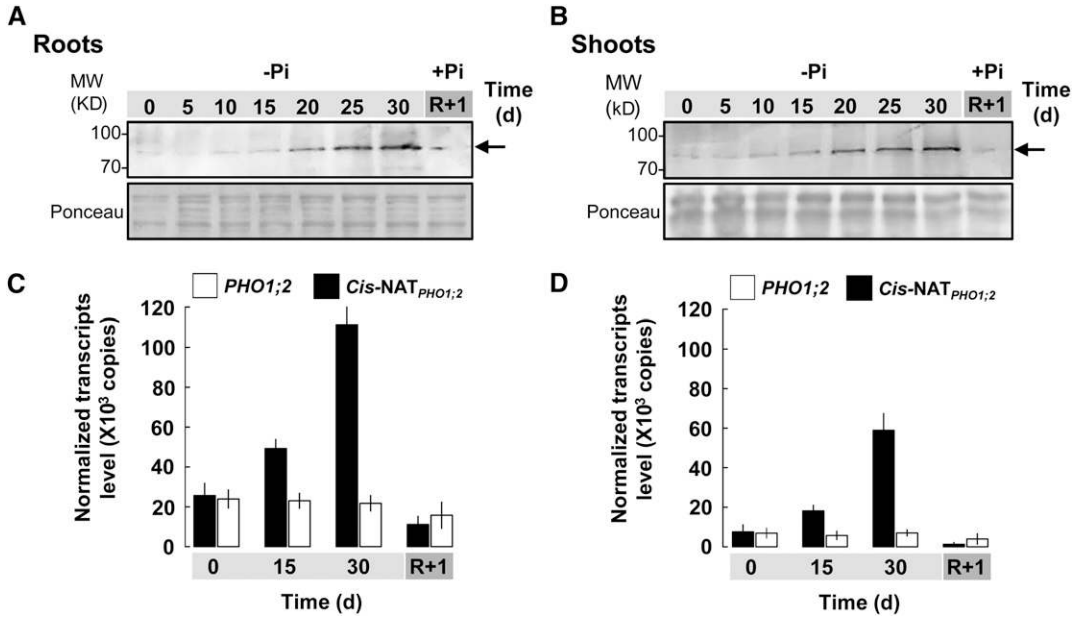

Figure 3. Analysis of the Relationship between *cis*-NAT$_{PHO1;2}$ Expression Level and PHO1;2 Protein Level.

(A) and **(B)** Immunoblot analysis of PHO1;2 protein synthesis in roots **(A)** or shoots **(B)** of wild-type plants grown in Pi-deficient medium from 0 to 30 d (−Pi, 0 to 30) or in Pi-deficient medium for 30 d followed by 1 d in medium with 1 mM Pi (+Pi, R+1). Fifty micrograms of microsomal proteins was loaded per lane. Immunoblots were probed with anti-OsPHO1;2 antibody. Ponceau S staining of the blot is shown in the bottom panel as a loading control. The position of PHO1;2 is indicated by the black arrow. MW, molecular mass.

(C) and **(D)** Expression analysis of *PHO1;2* and *cis*-NAT$_{PHO1;2}$ in roots **(C)** or in shoots **(D)** of the same plants used for immunoblot analysis. Strand-specific quantitative RT-PCR was performed to detect *PHO1;2* (white bar) and *cis*-NAT$_{PHO1;2}$ (black bar) transcripts level. The position of the primers used for quantitative RT-PCR is indicated in Figure 1A. Data are means ± SE (n = 3 to 4).

both roots and shoots, but no signal in shoots and only weak smeary signals in the root of the two RNAi lines, confirming the effectiveness and specificity of the RNAi construct toward *cis*-NAT$_{PHO1;2}$ (Figure 4G). Furthermore, wild-type plants grown under Pi starvation showed higher expression levels of *cis*-NAT$_{PHO1;2}$ transcript, consistent with previous findings.

Expression of certain *cis*-NATs has previously been shown to influence splicing of mRNA in regions of overlap between sense and antisense RNA (Hastings et al., 2000; Yan et al., 2005; Beltran et al., 2008). Although the RPA analysis described above showed only a full-length protected fragment for the sense *PHO1;2* transcript, indicating the absence of alternative splicing products, the presence of potential splicing variants was further analyzed by RT-PCR, using a combination of oligonucleotides bordering the exon-intron junctions for the first four exons of *PHO1;2*, the region overlapping with *cis*-NAT$_{PHO1;2}$ (Figure 4H). No alternative splicing was observed (Figure 4I). Furthermore, cDNA of *PHO1;2* using oligonucleotides that amplified the complete ORF region along with 174 and 356 bp of the 5′ and 3′ untranslated region (UTR), respectively, was also amplified from roots and shoots of the wild type and the two RNAi lines. Only a single PCR fragment of similar size was obtained for all samples (see Supplemental Figure 8 online). Direct DNA sequencing of the PCR products revealed identical nucleotide sequences for all samples, corresponding to *PHO1;2* full-length cDNA (based on the cDNA clone AK100323.1), with no evidence of a mixed population of cDNAs indicating the presence of splice variants. The presence of full-length *PHO1;2* transcript and the absence of splicing variants in the RNAi lines was also confirmed by RNA gel blot analysis using probes specific to the *PHO1;2* RNA and the *cis*-NAT$_{PHO1;2}$ (see Supplemental Figure 9 online). Taken together, these results reveal that a reduction of *cis*-NAT$_{PHO1;2}$ expression led to a reduction of PHO1;2 protein level without affecting the steady state level or splicing of the *PHO1;2* mRNA.

Double-stranded RNAs created by sense-antisense transcripts are potential substrates for RNA editing enzymes that lead to the deamination of either cytidine to create uridine or adenosine to create inosine (Bass, 2002; Meng et al., 2010). As such mRNA modifications could affect protein production by, for example, deleting or creating ATG start codons, the presence of edited transcript was examined in *PHO1;2* transcript from the wild type and the RNAi line Ri1. Five independent RT-PCR reactions were performed on RNAs from the wild type and the Ri1 line using oligonucleotides that amplify the region from the 5′ UTR to exon 5 of *PHO1.2*, which includes the region of overlap with *cis*-NAT$_{PHO1;2}$. Ten clones derived from each RT-PCR reaction were sequenced, for a total of 50 clones for the wild type and 50 clones for the Ri1 line. Sequences of all clones were identical, thus indicating that RNA editing is unlikely to contribute to the reduction in PHO1;2 protein triggered by the downregulation of *cis*-NAT$_{PHO1;2}$ expression.

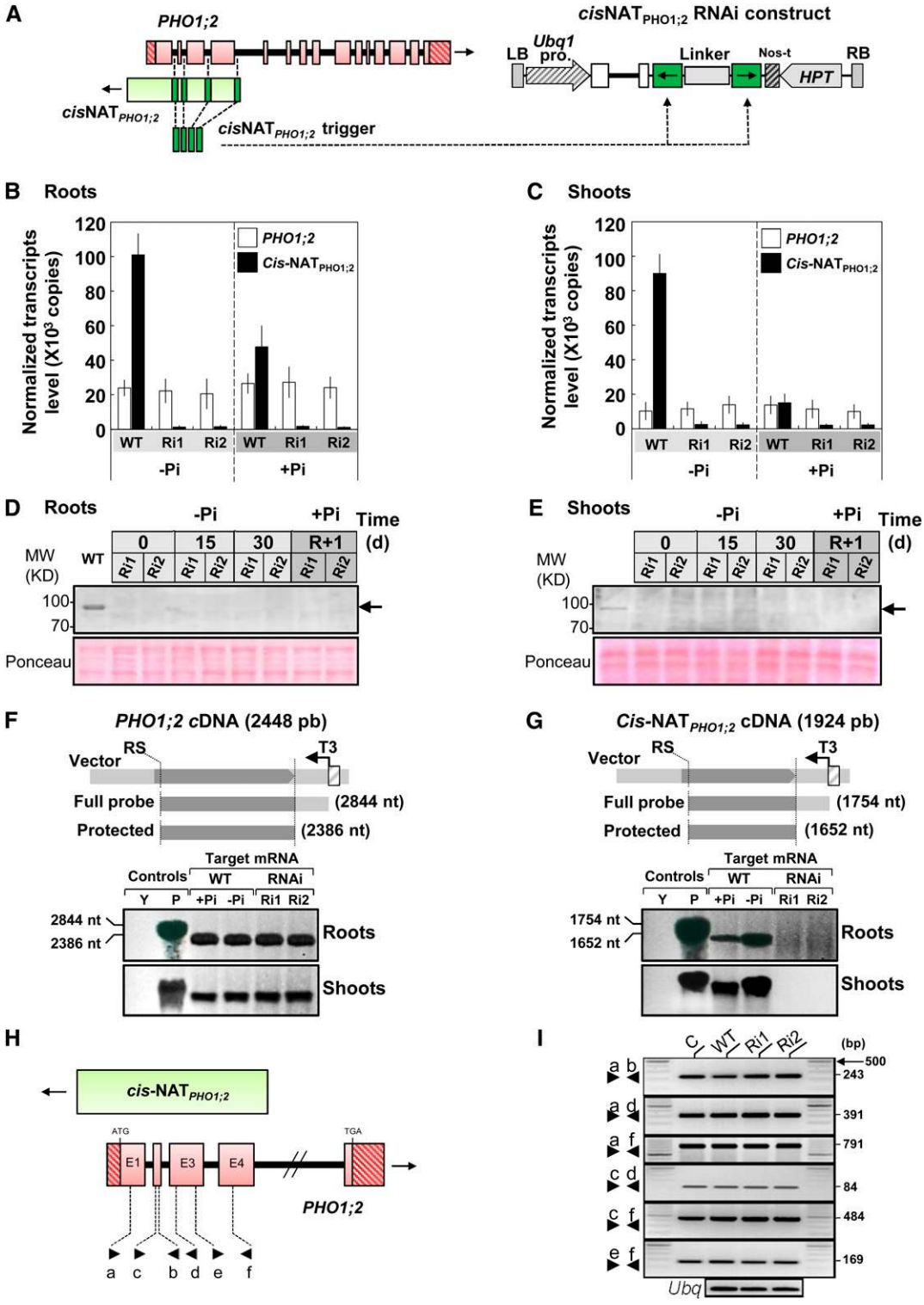

Figure 4. Modulation of *cis*-NAT$_{PHO1;2}$ Expression Affects PHO1;2 Protein Synthesis without Affecting Sense *PHO1;2* Transcript.

(A) Schematic diagram of the RNAi cassette in the pANDA-RNAi*cis*NAT$_{PHO1;2}$ construct. A chimeric 447-pb *cis*-NAT$_{PHO1;2}$ trigger was synthesized corresponding to four stretches of sequences (shown in dark green) that were present in *cis*-NAT$_{PHO1;2}$ transcript (pale and dark green) but absent from *PHO1;2* mRNA (plain red are exons and hatched red are untranslated sequences) (left diagram). The synthetic fragment was then cloned in two orientations in the pANDA vector to trigger RNAi (right diagram). The RNAi trigger was expressed constitutively under the control of the pUbq promoter

Overexpression of $NAT_{PHO1;2}$ in *Trans* Led to Increased PHO1;2 Protein Level

The link between $NAT_{PHO1;2}$ expression and PHO1;2 protein accumulation was further tested by overexpressing modified $NAT_{PHO1;2}$ containing epitope-tagged ORFs in shoots. Four transgenic lines were analyzed by quantitative RT-PCR and immunoblot analysis; two lines expressed only very low levels of transgenic $NAT_{PHO1;2}$ (lines OX26 and OX32), while lines OX8 and OX31 expressed high levels of transgenic $NAT_{PHO1;2}$ (Figure 2B). No change in the level of the sense *PHO1;2* transcript was observed among all lines tested (Figure 2B). By contrast, immunoblot analysis of microsomes from shoots indicated that while the wild type and lines OX26 and OX32 had comparable levels of PHO1;2 protein, lines OX8 and OX31 showed a strong increase in steady state PHO1;2 level (Figure 2D). These results indicated that overexpression of $NAT_{PHO1;2}$ in *trans* led to increased PHO1;2 accumulation.

Increased Expression of $NAT_{PHO1;2}$ Leads to Enhanced Association of Both Sense and Antisense Transcripts to Polysomes

To gain insight into the positive correlation between PHO1;2 production and expression of *cis*-$NAT_{PHO1;2}$, export of *PHO1;2* transcripts to the cytosol and its association with polysomes was examined. Comparison of transcripts present in a nuclear-enriched fraction compared with a cytosolic fraction indicated that more than 80% of both the *PHO1;2* and *cis*-$NAT_{PHO1;2}$ transcripts were found in the cytosolic fraction for all lines tested, which included the wild type, the RNAi lines Ri1 and Ri2, as well as the two $NAT_{PHO1;2}$-overexpressing lines OX31 and OX8 (see Supplemental Figure 10 online).

Polysome profiles were generated from roots of wild-type plants grown in Pi-sufficient or Pi-deficient media, as well as of roots of the RNAi lines Ri1 and Ri2 and the overexpressing lines OX8 and OX31 grown in Pi-sufficient medium (Figure 5). Wild-type plants grown in Pi-deficient medium showed a clear enrichment of the *PHO1;2* mRNA in the heavy polysome fraction compared with wild-type plants grown in Pi-sufficient medium (Figure 5A). No similar shift toward the heavier polysomal fraction was observed for transcripts of the *PHO1;3* homolog (Secco et al., 2010), indicating a specificity of the polysomal enrichment for *PHO1;2* mRNA. Similarly, for plants grown in Pi-sufficient media, an enrichment of *PHO1;2* transcript in the polysomal fractions was observed for the OX lines compared with the wild type, while a reduction was observed for the RNAi lines (Figure 5B). Interestingly, the distribution of *cis*-$NAT_{PHO1;2}$ in both the wild type and the OX lines followed the same trend as for the sense *PHO1;2* transcript, being enriched in the polysome fraction in Pi-deficient wild-type plants and in Pi-sufficient OX plants (Figure 5C). Furthermore, in the OX lines, the transgenic epitope-tagged NAT transcript was also enriched in the polysome fractions (Figure 5C). These data reveal that the increased expression of a $NAT_{PHO1;2}$ transcript, triggered either by phosphate deficiency or via transgenesis, leads to a shift of both the sense *PHO1;2* and the antisense NAT toward the translationally active polysomes.

Effect of *cis*-$NAT_{PHO1;2}$ Suppression on Plant Growth and Pi Homeostasis

To understand the role of the endogenous *cis*-$NAT_{PHO1;2}$ on plant growth and Pi homeostasis, the effect of a reduction of *cis*-$NAT_{PHO1;2}$ expression was analyzed in the RNAi lines Ri1 and Ri2. Growth and Pi content were assessed for the RNAi lines, the null mutant *pho1;2* (Secco et al., 2010), and wild-type plants grown hydroponically under Pi-sufficient or Pi-deficient conditions for 4 weeks. Growth of the RNAi lines was indistinguishable from that of the wild type over the early vegetative period, whereas the *pho1;2* mutant showed a net decrease in shoot and root biomass compared with the wild type (Figures 6A and 6B). Yet, in contrast with the near-wild-type growth behavior of the RNAi lines, the assessment of the steady state Pi levels from plants grown in Pi-deficient media showed differences between RNAi lines and wild-type plants (Figures 6C and 6D). Under this condition, the RNAi plants had approximately twofold less Pi in the shoots and threefold more Pi in the roots compared with the wild-type plants (Figures 6C and 6D). By contrast, under Pi-sufficient conditions, the RNAi mutants showed no significant difference in shoot or root

Figure 4. (continued).

of the maize ubiquitin gene. Downstream of pUbq, the two unlabeled boxes represent exons and the thick line separating the exons marks an intron of the *Ubq* gene.

(B) and **(C)** Quantitative RT-PCR analysis of *PHO1;2* and *cis*-$NAT_{PHO1;2}$ transcripts in roots **(B)** and shoots **(C)** of wild-type (WT) plants and RNAi lines (Ri1 and Ri2) grown in Pi-deficient or Pi-sufficient conditions. Data are means ± SE (n = 5).

(D) and **(E)** Immunoblot analysis of PHO1;2 synthesis in roots **(D)** or shoots **(E)** of wild-type plants and RNAi lines grown under Pi-deficient or Pi-sufficient conditions. Microsomal proteins were extracted at different time points during the Pi starvation (0, 15, and 30 d) and 1 d after Pi recovery (R+1). As a control, 30-d-old wild-type plants were used. Immunoblots were probed with anti-OsPHO1;2 antibody. Ponceau S staining of the blot is shown in the bottom panel as a loading control. The position of PHO1;2 is indicated by the black arrow. MW, molecular mass.

(F) and **(G)** RPA analysis of *PHO1;2* **(F)** or *cis*-$NAT_{PHO1;2}$ **(G)** transcripts in wild-type plants and RNAi lines. A schematic representation of ^{32}P-labeled full-length single-stranded RNA probes used to detect both the sense *PHO1;2* RNA and *cis*-$NAT_{PHO1;2}$ is shown in the top panels. Autoradiographs revealing the hybridizations corresponding to the undigested probe (P) (1% of the amount used in the RPA) as well as the protected fragments in both roots and shoots are shown in the bottom panels. Yeast tRNA (Y) was used as a negative control. nt, nucleotides.

(H) and **(I)** Alternative splicing analysis of the 5′-coding region of *PHO1;2* by RT-PCR.

(H) Map of the relative primer positions (arrowheads) used in alternative splicing analysis shown in **(I)**.

(I) Analysis of RT-PCR products resulting from amplification across all four exons E1 to E4 in wild-type and RNAi lines. The rice ubiquitin gene (Ubq) was used as internal control, and DNA plasmid containing full-length *PHO1;2* cDNA was used as a positive control (C). The figure shows a typical result from a duplicate technical replicate.

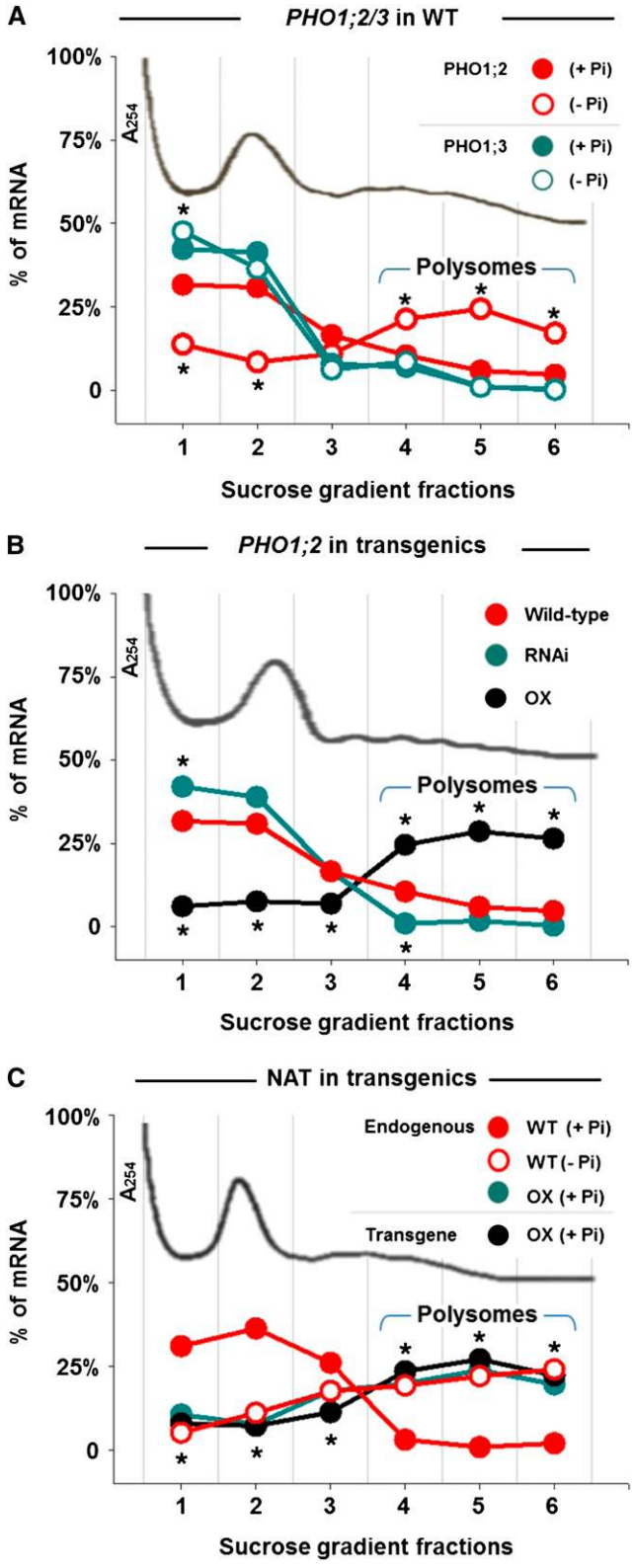

Figure 5. Increased Polysome Association of *PHO1.2* mRNA upon Pi Deficiency Treatment or $NAT_{PHO1;2}$ Overexpression.

Quantitative RT-PCR was performed on root RNAs purified from six Suc gradient fractions to quantify transcripts from *PHO1;2* and *PHO1;3* in wild-type (WT) plants grown in Pi-sufficient or Pi-deficient media **(A)**, *PHO1;2* in the wild type, in the *cis*-$NAT_{PHO1;2}$ RNAi lines Ri1 and Ri2, and in the lines OX8 and OX32 overexpressing a modified $NAT_{PHO1;2}$, with all plants grown in Pi-sufficient medium **(B)**, and the endogenous *cis*-$NAT_{PHO1;2}$ in wild-type plants grown on Pi-sufficient or Pi-deficient media, and both the endogenous and transgenic $NAT_{PHO1;2}$ in the OX8 and OX32 lines grown on Pi-sufficient conditions **(C)**. Data obtained for the two RNAi lines or the two OX lines were similar and thus pooled to simplify the graphical display. The association with each fraction is shown as a linear plot of the percentage of RNA present in each fraction; the plot is superimposed on a representative absorbance profile of the gradient. Fractions representing polysomes are indicated by a bracket. Statistically significant differences relative to either *PHO1;2* for the +Pi treatment in **(A)**, *PHO1;2* for the wild type in **(B)**, or endogenous *cis*-$NAT_{PHO1;2}$ for the +Pi treatment in **(C)** are indicated by asterisks (*t* test, $P < 0.05$, $n = 3$). For **(C)**, the asterisks apply to all three points in close proximity.

Pi content compared with the wild type. The assessment of Pi transfer from the root to shoot in plants grown in Pi-deficient medium revealed a 1.7-fold reduction in the RNAi lines compared with the wild type (Figure 6E). However, the decrease was smaller than for the *pho1;2* null mutant (Figure 6E). These results indicate that a low level of PHO1;2 expression must be present in the RNAi lines that is sufficient to maintain a shoot Pi level similar to that in wild-type plants grown in Pi-sufficient conditions, but not for plants grown under Pi-deficient conditions.

For phenotypic observation during the entire plant growth period, experiments were performed with soil-grown plants. Plants were grown for 5 to 6 months with regular Pi fertilization and the phenotypes were examined. At the heading stage, RNAi lines showed no phenotypic differences compared with nontransformed rice plants, and the biomass of roots and shoots was comparable (Figures 7A and 7B). However, as previously observed during the early vegetative phase, Pi distribution between shoots and roots of the RNAi lines was strongly affected compared with wild-type plants (Figure 7C). Pi level was strongly increased in roots and decreased in shoots. Moreover, seed-setting rate was decreased in RNAi lines (Figure 7D, top panel) and grains were smaller and thinner compared with wild-type plants (Figures 7D and 7E). Altogether, these data demonstrate that *cis*-$NAT_{PHO1;2}$ acts as a positive regulator of Pi homeostasis through increased *OsPHO1;2* mRNA translation.

DISCUSSION

In contrast with small ncRNAs (siRNAs and miRNAs), which generally have conserved structures and are involved in gene silencing via specific base-pairing with their target, the long ncRNAs do not share conserved features and are implicated in diverse mechanisms of gene regulation. Although only a limited number of long ncRNAs have been characterized in some detail in plants, fungi, and metazoans, the majority have been shown to affect mRNA transcript levels (Au et al., 2011; Kim and Sung, 2012; Rinn and Chang, 2012). Long ncRNAs involved in the repression of transcription are predominant and implicate diverse mechanisms,

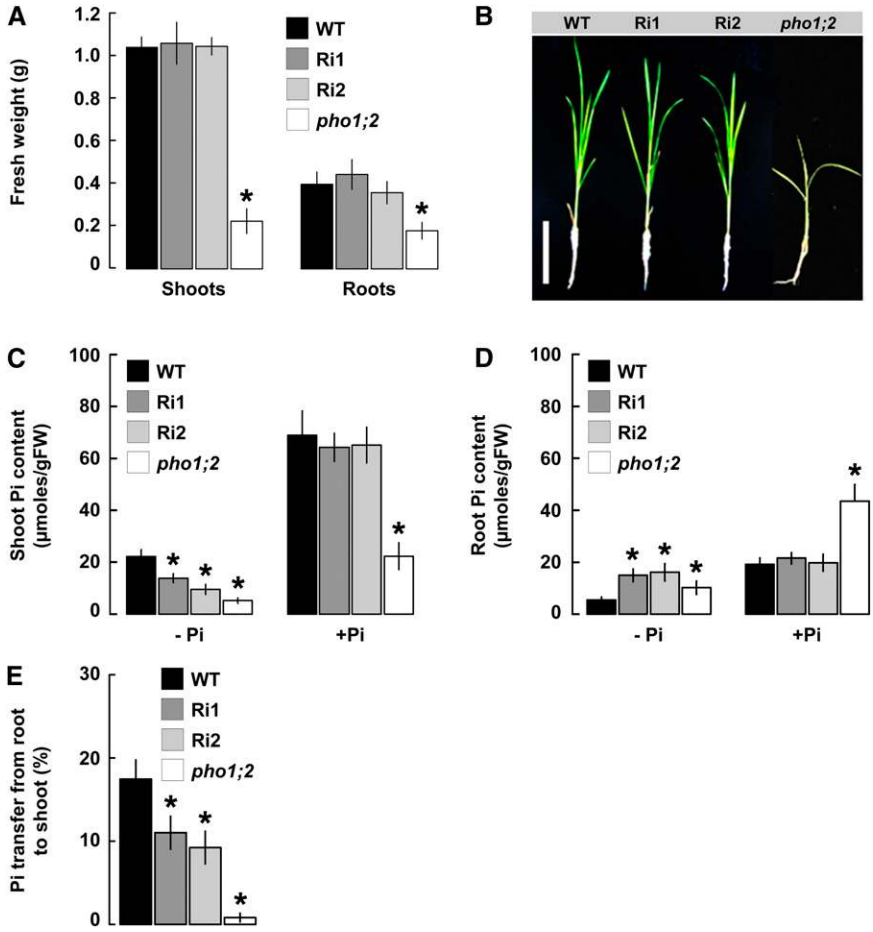

Figure 6. Phenotypic Analysis of the *cis*NAT$_{PHO1;2}$ RNAi Lines.

(A) Fresh weight of shoots and roots of RNAi lines, *pho1;2*, and the wild type (WT) after 4 weeks of growth in Pi-sufficient medium.
(B) Morphological appearance of 30-d-old wild-type, *pho1;2*, and RNAi lines grown hydroponically in Pi-sufficient medium.
(C) and **(D)** Pi content assessed in shoots **(C)** and roots **(D)** of RNAi lines, *pho1;2*, and wild-type plants. FW, fresh weight.
(E) Transfer rate of ^{33}P from roots to shoots of 3-week-old plants grown hydroponically in Pi-deficient medium.
Data are mean ± SE ($n = 5$), except for **(E)** ($n = 4$). Asterisks indicate statistically significant differences relative to the wild-type control (*t* test, $P < 0.05$). [See online article for color version of this figure.]

such as the recruitment of proteins modifying histone structure for *X INACTIVE SPECIFIC TRANSCRIPT* and *HOTAIR* in mammals (Rinn et al., 2007; Zhao et al., 2008) or *COOLAIR* in plants (Swiezewski et al., 2009), titrating transcription factors for *PANDA* or *DIHYDRFOLATE REDUCTASE MINOR* in mammals (Martianov et al., 2007; Hung et al., 2011) or transcriptional interference for *INTERFERING CRIC RNA1* and *ZIPPING2* in yeast (Bumgarner et al., 2009; Gelfand et al., 2011). A reduction of steady state mRNA levels by long ncRNAs has also been described that implicates posttranscriptional mechanisms, such as mRNA degradation via half-STAU1 binding sites in mammals (Gong and Maquat, 2011) or siRNA via Dicer and double-stranded sense-antisense duplexes in plants, *Drosophila*, and mammals (Katiyar-Agarwal et al., 2006; Held et al., 2008; Okamura et al., 2008; Watanabe et al., 2008). Long ncRNAs have also been implicated in increasing steady state levels of target mRNA, either by increasing transcription by chromatin remodeling, as for *HOTTIP* in mammals (Wang et al., 2011) and long ncRNAs that act as enhancers (Ørom et al., 2010), or by increasing mRNA stability, such as in the case of *BETA-SECRETASE1* (Faghihi et al., 2008).

Cases where long ncRNAs affect protein level without corresponding changes in steady state mRNA are relatively rare, and none have been reported in plants. One example in mammals is the translational inhibition of the mRNA encoding the transcription factor PU.1 by its associated *cis*-NAT (Ebralidze et al., 2008). There are also a few cases where long ncRNAs, and particularly *cis*-NATs, regulate protein expression via mRNA splicing, such as the regulation of ZINC FINGER E-BOX BINDING HOMEOBOX2 expression in mammals through inhibition of the splicing of an intron containing a ribosome entry site (Beltran et al., 2008) and the control of alternative splicing variants of the apoptotic factor APOPTOSIS STIMULATING FRAGMENT (Yan et al., 2005). Recently, a unique example of a *cis*-NAT that enhances protein expression independently of mRNA level has

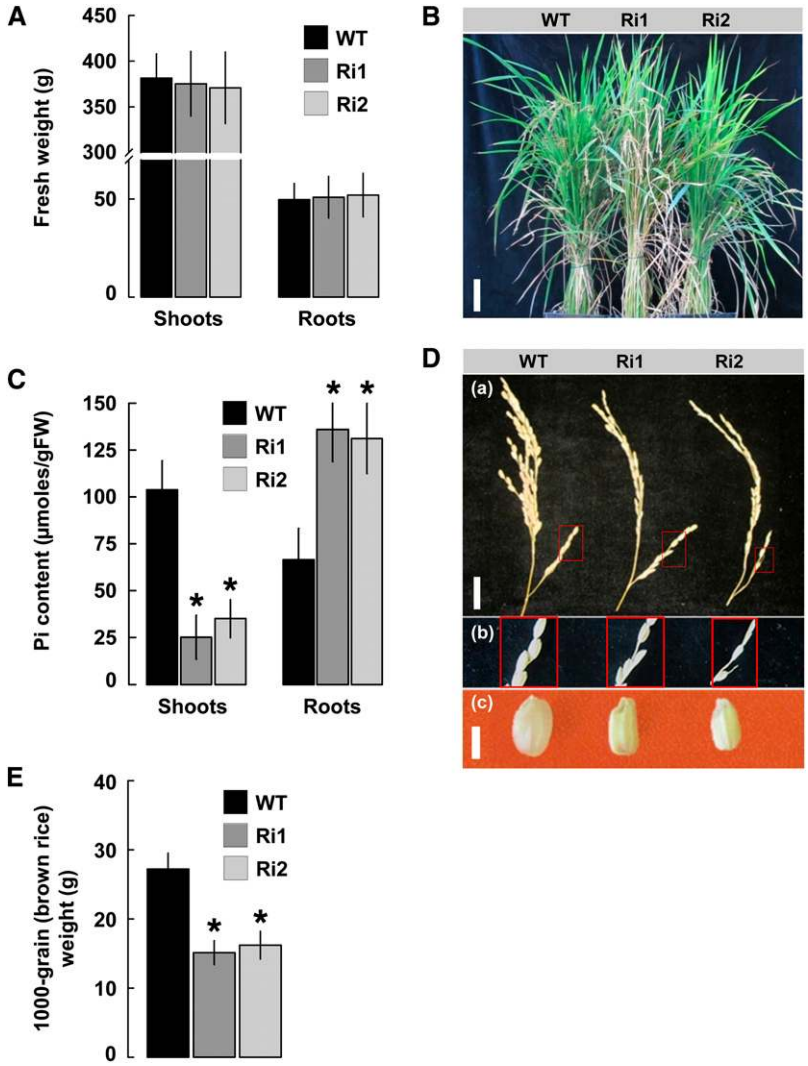

Figure 7. Phenotypic Analysis of the RNAi Lines at Maturity.

Measurements were made on rice plants grown for 6 months in a greenhouse under a day/night temperature regime of 30°C/25°C. Plants were fertilized weekly with a nutrient solution containing 1 mM Pi.

(A) Shoot and root biomass in wild-type (WT) and transgenic plants.

(B) Morphology at the heading stage of wild-type plants, RNAi-line1 (Ri1), and RNAi-line2 (Ri2). Bar = 10 cm.

(C) Pi content assessed in roots and shoots of RNAi lines and wild-type plants. Data are mean ± SE (n = 4). FW, fresh weight.

(D) Comparison of panicle-filling performance and seed phenotype at harvest of RNAi lines and wild-type plants. Inset (a), seed-setting performance in RNAi lines and the wild type. Inset (b), magnified view of spikelet (boxed in [a]) on the primary rachis branch of the wild type (left), Ri1 (center), and Ri2 (right). Inset (c), comparison of the brown rice seeds. Bars = 0.25 cm.

(E) Weight of 1000 grains of wild-type and RNAi lines. All data are mean ± SE (n = 7 to 10). Asterisks indicate statistically significant differences relative to the wild-type control (t test, $P < 0.05$).

[See online article for color version of this figure.]

been described in mammals (Carrieri et al., 2012). Expression of the *cis*-NAT associated with the mouse *UBIQUITIN CARBOXY-TERMINAL HYDROLASE L1* (*Uchl1*) gene was shown to increase UCHL1 synthesis without changes in its transcript level. This activity of the *cis*-NAT was dependent on the presence of a 5′ base pairing with its cognate mRNA and of an inverted short interspersed nuclear element (SINEB2) at the 3′ end and could occur by expression of these elements in *trans*. It was proposed that the association of *Uchl1* mRNA with its *cis*-NAT in the cytosol enhances its translation.

The expression pattern of the promoter of Os-*PHO1;2* in the vascular cylinder is comparable to the expression pattern of the homologous At-*PHO1* promoter in the same tissues in *Arabidopsis* roots and in agreement with the characterized role of Os-PHO1 and At-PHO1 in the transfer of Pi into the xylem vessel (Hamburger et al., 2002; Secco et al., 2010). The promoter of

Os-*PHO1;2* is marginally responsive to the Pi status of the plant, in agreement with a lack of change in Os-*PHO1;2* transcript expression upon Pi deficiency. By contrast, the *cis*-$NAT_{PHO1;2}$ promoter activity is strongly increased upon Pi deficiency and correlates with a marked increase in *cis*-$NAT_{PHO1;2}$ transcript level under the same conditions, indicating a major transcriptional regulation of *cis*-$NAT_{PHO1;2}$ expression by the Pi status. An analysis of the sequence of the *cis*-$NAT_{PHO1;2}$ promoter did not reveal the presence of P1BS-like elements (GNATATNC) recognized by PHR1, a major transcription factor responsible for the transcriptional upregulation of numerous genes under Pi deficiency (Rubio et al., 2001). Thus, further work is needed to identify the *cis*-regulatory elements responsible for the transcriptional regulation of *cis*-$NAT_{PHO1;2}$. Importantly, the expression pattern of the *cis*-$NAT_{PHO1;2}$ promoter overlapped with the expression of the *PHO1;2* promoter in both the shoot and root vascular cylinder, an important element for a regulatory role of *cis*-$NAT_{PHO1;2}$ on PHO1;2 expression.

Three lines of evidence support the conclusion that *cis*-$NAT_{PHO1;2}$ positively regulates PHO1;2 protein accumulation without affecting steady state mRNA level. First, time-course analysis during Pi deficiency stress showed strong correlation between *cis*-$NAT_{PHO1;2}$ transcript level and PHO1;2 protein accumulation. Second, specific downregulation of *cis*-$NAT_{PHO1;2}$ via RNAi led to a strong decrease in PHO1;2 protein accumulation under Pi-sufficient and Pi-deficient conditions. Third, overexpression of a modified $NAT_{PHO1;2}$ in transgenic plants caused an increased PHO1;2 protein accumulation. Importantly, under all experimental conditions tested, no significant changes occurred in *PHO1;2* steady state mRNA level.

The RNAi strategy used in this work relied on the expression of a chimeric construct composed of sequences corresponding to the exon of the *cis*-$NAT_{PHO1;2}$ transcript but only to introns of the sense transcript (Figure 4A). Expression of this RNAi construct resulted in the selective degradation of only the *cis*-$NAT_{PHO1;2}$ mRNA, revealing that RNAi-mediated transcript degradation only targeted mature transcripts and not the nuclear pre-mRNA *PHO1;2* transcript containing introns. These results are in contrast with previous work showing siRNA-directed degradation of the *FATTY ACID DESATURASE2-1A* transcript in soybean (*Glycine max*) using an RNAi construct containing only intronic sequences to the target gene (Hoffer et al., 2011). While ARGONAUTE-mediated target cleavage has been shown to occur in the nucleus in *Schizosaccharomyces pombe*, the subcellular location of ARGONAUTE loading in plants remains unclear (Castel and Martienssen, 2013). Our results imply that there are probably differences either between plant species or between genes in their sensitivity to siRNA-mediated degradation in the cytosol or the nucleus.

Analysis by RPA and RT-PCR of the *PHO1;2* transcripts in plants grown under conditions of high or low *cis*-$NAT_{PHO1;2}$ expression level did not reveal any evidence of alternative splicing or editing of the *PHO1;2* transcript. Furthermore, analysis of databases of cDNAs, ESTs, or whole-genome RNA sequencing from rice also did not reveal the presence of alternative splicing products for *PHO1;2*. Thus, expression of *cis*-$NAT_{PHO1;2}$ is unlikely to affect PHO1;2 production via modification of the *PHO1;2* transcript. Instead, *cis*-$NAT_{PHO1;2}$ expression has a clear role in increasing PHO1;2 production by enhancing the association of mRNA with polysomes. The fact that polysome association of *PHO1;2* was stimulated not only by the increased expression of *cis*-$NAT_{PHO1;2}$ in Pi-deficient wild-type plants, but also by the overexpression, in *trans*, of $NAT_{PHO1;2}$ in Pi-sufficient plants, reveals that $NAT_{PHO1;2}$ can positively regulate PHO1;2 synthesis independently of the metabolic and development changes that accompany Pi deficiency and that this regulation does not require a *cis*-configuration of the sense and antisense transcripts. Future work will need to focus on the mechanism by which *cis*-$NAT_{PHO1;2}$ can enhance the association of the *PHO1;2* transcript with polysomes. One attractive hypothesis is that *cis*-$NAT_{PHO1;2}$ associates with *PHO1;2* via its overlapping region and that the free 3′ end of *cis*-$NAT_{PHO1;2}$ can recruit initiation factors or ribosomes that will then be translocated to the 5′ end of the *PHO1;2* transcript. This hypothesis would fit the observation that $NAT_{PHO1;2}$ is also found in the polysome fraction. Such a model would be reminiscent of the translational enhancers found at the 3′ UTR region of several plant RNA viruses (Simon and Miller, 2013).

Studies of the role of *cis*-NATs in the regulation of gene expression in plants have so far identified two main mechanisms. Downregulation of the target mRNA level via siRNAs appears predominant, with examples of siRNA generated from sense−*cis*-NAT double-stranded RNA being implicated in the response of plants to salt stress or pathogen infection, cellulose biosynthesis, flowering control, sperm cell development, and cytokinin biosynthesis (Borsani et al., 2005; Katiyar-Agarwal et al., 2006; Swiezewski et al., 2007; Zubko and Meyer, 2007; Held et al., 2008; Ron et al., 2010). A second mechanism described for only *FLC* is the transcriptional downregulation of mRNA synthesis by the recruitment of chromatin modifying protein and histone methylation (Swiezewski et al., 2009; Liu et al., 2010; Heo and Sung, 2011). Despite the apparent prevalent role of siRNA in mediating the downregulation of gene expression by *cis*-NATs in the literature, a recent genome-wide analysis of siRNAs in biotic and abiotic stress–challenged *Arabidopsis* and rice found that only 6.1 and 15.7% of the *Arabidopsis* and rice sense−*cis*-NAT pairs, respectively, gave rise to significant levels of siRNAs (Zhang et al., 2012). Similar studies performed for rice and six other plants found that while siRNAs were particularly enriched in the overlapping regions of *trans*-NATs, only low levels of enrichment were found for *cis*-NATs (Zhou et al., 2009; Chen et al., 2010). Together, these studies reveal that siRNA-mediated gene silencing is unlikely to be the main mechanism by which *cis*-NATs regulate gene expression. This work on *cis*-$NAT_{PHO1;2}$ thus highlights a novel mode of regulation of *cis*-NATs on their sense targets in plants that may be of relevance to other sense−*cis*-NAT pairs, in particular those that show no correlation between *cis*-NAT induction and the negative effect on the sense mRNA transcript.

The physiological importance of *cis*-$NAT_{PHO1;2}$ action is shown in the RNAi lines that have a specific decrease in *cis*-$NAT_{PHO1;2}$ expression. Indeed, these RNAi lines show reduced transfer of Pi from root to shoot, leading to a reduction in shoot Pi and a concomitant increase in root Pi content. The fact that decreased PHO1 activity and shoot Pi content did not affect shoot biomass production for plants grown in well-fertilized soil is fully consistent with previous results obtained in *Arabidopsis* showing that it is possible to uncouple low shoot Pi content from reduced shoot growth by modulating the expression of PHO1 (Rouached et al., 2011). However, our results show that rice lines with reduced *cis*-$NAT_{PHO1;2}$ expression show a severe reduction in seed yield

and seed weight, highlighting the important role of *cis*-NAT$_{PHO1;2}$ in plant fitness.

The plant's response to Pi deficiency is already known to implicate two ncRNAs. One is miR399, an miRNA induced by Pi deficiency that targets the *PHO2* transcript, which encodes a ubiquitin-conjugating E2 enzyme that interacts with PHO1 and promotes its degradation (Lin et al., 2008; Pant et al., 2009; Liu et al., 2012). IPS1 is another ncRNA that is induced under Pi deficiency and acts as a target mimic for miR399, thus providing a level of feedback control over miR399 action (Franco-Zorrilla et al., 2007). This work on *cis*-NAT$_{PHO1;2}$ adds an additional layer of complexity and reveals an important role for a *cis*-NAT in the regulation of PHO1 activity and phosphate homeostasis.

METHODS

Plant Material and Growth Conditions

Rice (*Oryza sativa* ssp *japonica* 'Nipponbare') was used for all experiments. For hydroponic culture, seeds were first surface sterilized and germinated as described previously (Jabnoune et al., 2009). For plants grown under Pi deficiency, 7-d-old seedlings were grown in full-strength Hoagland nutrient solution (1 mM Pi) and then subjected to Pi deficiency (0 mM Pi, KH_2PO_4 was replaced by KCl) or the control condition (1 mM Pi) for the desired time duration. In experiments involving transgenic plants, seeds were geminated and screened in a solution containing 50 mg L^{-1} hygromycin for 7 d and then confirmed by PCR for the presence of the transgene before being transferred to the hydroponic system. Growth conditions were 28°C, 13-h-light/22°C, 11-h-dark cycle in a phytotron or 30°C, 12-h-light/22°C, 12-h-dark cycle in a greenhouse.

Plasmid Construction and Plant Transformation

To develop transgenic plants expressing the GUS reporter gene, 2 kb of the promoter sequence of *PHO1;2* and *cis*-NAT$_{PHO1;2}$ were cloned into the vector pHGWFS7.0 (Karimi et al., 2002). To develop transgenic plants expressing an RNAi construct targeting *cis*-NAT$_{PHO1;2}$, a synthetic DNA fragment containing the sequence of the first, second, and third introns of *PHO1;2* was synthesized (Invitrogen) and cloned into the pANDA vector containing the maize (*Zea mays*) ubiquitin promoter region (Miki and Shimamoto, 2004). To generate transgenic plants overexpressing a modified NAT$_{PHO1;2}$ with epitope-tagged ORFs, a synthetic NAT$_{PHO1;2}$ fragment was synthesized (Invitrogen) containing the FLAG, HA, and MYC epitopes inserted at the 3′ end of ORF1, ORF2, and ORF3, respectively. The modified NAT$_{PHO1;2}$ construct was introduced into the expression vector pMDC32 harboring the cauliflower mosaic virus 35S promoter (Curtis and Grossniklaus, 2003). All the constructs described above were introduced into rice by *Agrobacterium tumefaciens*–mediated transformation at the Iowa State University Plant Transformation Facility. To express each epitope-tagged NAT$_{PHO1;2}$ ORF separately into *Escherichia coli*, DNA fragments corresponding to each tagged ORF were amplified from the synthetic NAT$_{PHO1;2}$ fragment and cloned into the expression vector pLATE11 (Thermo Scientific).

Histochemical GUS Staining and Fluorometric Assays

Plant tissues were collected from wild-type and transgenic plants containing the Pro$_{OsPHO1;2\text{-}S}$:GUS or Pro$_{cis\text{-}NAT}$:GUS transgenes. The root and leaf sections were vacuum infiltrated in X-gluc solution [0.5 mM X-gluc, 0.1 M $NaHPO_4$, pH 8.0, 0.5 mM $K_3Fe(CN)_6$, 0.5 mM $K_4Fe(CN)_6$, 0.01 M EDTA, pH 8.0, 20% methanol, and 0.1% Triton X-100] twice for 5 min each, followed by incubation at 37°C for 16 h and cleared two or three times with 70% ethanol at 65°C before samples were whole mounted in 70% ethanol for microscopy. For cross sections, the stained samples (without clearing) were embedded in 4% agarose, and 50-μm sections were made using a Vibratome (Leica VT1000 S).

Quantitative GUS activity was determined by measuring the production of 4-methylumbelliferone. For this, five samples from lines transformed with each construct were pooled and used for a quantitative 4-methylumbelliferyl-β-D-glucuronide assay. Plant tissues were homogenized in 0.4 mL of protein extraction buffer (0.1 M $NaPO_4$, pH 8.0, 0.1% SDS, 10 mM EDTA, 10 mM β-mercaptoethanol, and 0.1% Triton X-100) followed by centrifugation at 13,000*g* and 4°C for 15 min. The supernatant was used for protein quantification and fluorometric assay. Fifty microliters of supernatant was transferred to a microcentrifuge tube containing 500 μL of GUS reaction buffer (protein extraction buffer containing 10 mM 4-methylumbelliferyl-β-D-glucuronide) prewarmed to 37°C and mixed. One hundred microliters of this mixture was immediately transferred into 900 μL of GUS stop buffer (0.2 M Na_2CO_3) to serve as a control. The sample reaction mixture was incubated at 37°C. One hundred microliters of aliquots was removed at 15-, 30-, 60-, and 120-min intervals and mixed with 900 μL of GUS stop buffer. GUS activity was measured in a fluorometer (VersaFluor; Bio-Rad) with excitation at 365 nm and emission at 455 nm. The amount of 4-methylumbelliferone was determined from a standard curve. Protein concentrations of the samples were determined using Bradford reagent (Bio-Rad) and BSA as a standard.

RNA Extraction and Transcript Analysis

Total RNA was extracted using an RNeasy plant mini kit (Qiagen) following the manufacturer's instructions. cDNA was synthesized from 1 μg of DNaseI-treated total RNA (Fermentas) using oligo(dT) and Moloney murine leukemia virus reverse transcriptase (Promega) according to the manufacturer's instructions. Strand-specific real-time PCR was performed in a 25-μL volume containing 5 μL of cDNA, 12.5 μL of 2× SYBR green mix (Axon Lab), and 0.25 μM each primer. Analysis was performed in an MX3000P real-time PCR system (Stratagene) with cycle conditions of an initial denaturing at 95°C for 15 min, followed by 40 cycles of 95°C for 30 s, 60°C for 1 min, and 72°C for 1 min. The transcript-specific primers used are listed in Supplemental Table 1 online. All data were normalized against the expression level of the rice ubiquitin gene.

Protein Preparation and Immunoblot Analysis

For extraction of the microsomal protein fractions, tissues from roots or shoots of wild-type or mutants plants were frozen in liquid nitrogen and ground with a mortar and pestle. The frozen powder was homogenized with three volumes of ice-cold extraction buffer composed of 100 mM Tris-HCl, pH 7.5, 400 mM Suc, 1 mM EDTA, 0.1 mM phenylmethylsulfonyl fluoride, and 1× complete protease inhibitor (Roche). Debris was pelleted by centrifugation at 1000*g* for 5 min (at 4°C). The pellet was discarded and the supernatant was centrifuged at 8000*g* for 15 min (at 4°C). The pellet was discarded and the supernatant was recentrifuged at 150,000*g* for 1 h, at 4°C, to produce a 150,000*g* membrane pellet (P150) and a soluble fraction (S150). The P150 pellets were resuspended in standard extraction buffer supplemented with 0.5% (v/v) Triton X-100 and were used as crude microsomal membranes. The protein concentration was determined by DC protein assay (Bio-Rad) according to the manufacturer's instructions using an Epoch Micro-Volume Spectrophotometer system (Biotech Systems). Equal amounts of proteins (50 to 80 μg) were used for immunoblot analyses.

Proteins were separated by 4 to 20% Mini-Protean TGX gels (Bio-Rad) and transferred to polyvinylidene difluoride membrane (Hypobond-PVDF; Amersham Lifesciences) by electroblotting in transfer buffer (25 mM Tris, 192 mM Gly, and 10% methanol, pH 8.3). Nonspecific binding was reduced with blocking solution (5% [w/v] BSA in 1× PBS-Tween-20 [1× PBST solution], pH 7.2) at room temperature for 1 h with agitation. Then,

blots were hybridized with a rabbit polyclonal antibody against PHO1;2 diluted 1:10,000 in 1× PBST overnight (at 4°C) with agitation. After three washes for 15 min in 1× PBST, blots were incubated with the secondary antibody (rabbit IgG; Sigma-Aldrich) for 1 h at room temperature. Three further washing steps (15 min each) in PBS were followed by detection using an Enhanced Chemiluminescence Plus detection kit (enhanced chemiluminescence protein gel blotting detection; GE Healthcare) and the ImageQuant 300 imager (GE Healthcare). The protein transferred onto membranes was visualized with Ponceau staining solution (0.1% [w/v] Ponceau S and 5% [v/v] acetic acid).

Rabbit primary polyclonal antibody was raised against the N-terminal fragment of PHO1;2 corresponding to the amino acid residues 78 to 177 (Strategic Diagnostics) and was affinity purified using immunogenic peptide coupled to a SulfoLink column (Pierce).

Recombinant Protein Production in *E. coli*

The plasmids were transformed in *E. coli* strain BL21(DE3) cells, and the induction of recombinant protein expression was performed by adding 0.5 mM isopropyl β-D-1-thiogalactopyranoside (37°C, 3 h) to the growth medium.

RNase Protection Assay

Total RNA was extracted from rice roots or shoots using an RNeasy plant mini kit (Qiagen) following the manufacturer's instructions. RPAs were performed as described previously with some modifications (Young et al., 2003). To prepare cRNA probes specific for *PHO1;2* or *cis*-$NAT_{PHO1;2}$, the full-length cDNA of *PHO1;2* and *cis*-$NAT_{PHO1;2}$ was first subcloned into the pFLCI vector, and then the plasmid was linearized by *Sma*I (OsPHO1;2-AS-pFLCI) or *Sal*I (OsPHO1;2-S-pFLCI). The linearized fragments were used as templates to generate a ^{32}P-labeled antisense ripoprobes using T3 RNA polymerase, [α-^{32}P]rCTP (10 mCi/mL), and the Riboprobe transcription kit (Promega) according to the manufacturer's instructions.

Before conducting nuclease protection assays, ribonucleotide probes were extracted with phenol:chloroform (1:1) and then chloroform. Unincorporated nucleotides were removed with a G-50 Sephadex column (Roche Molecular Biochemicals). Total RNA was hybridized to 3×10^5 cpm of labeled antisense probe and subsequently treated with RNase A and RNase T1 to digest unhybridized probe and single-stranded RNA. Digestion was stopped, and hybridized RNA was precipitated by the addition of RNase inactivation/PPT reagent III (Ambion) and incubation for 30 min at −20°C. Hybridized RNA was pelleted by centrifugation at 14,000*g* for 15 min. Protected mRNA fragments were identified by their electrophoretic mobility through a 5% acrylamide, 8 M urea denaturating gel (250 V for 1 h). Gels were dried and autoradiography was performed using x-ray film (Biomax-MR; Kodak) for 24 to 48 h at −80°C with intensifying screens.

RNA Gel Blot Analysis

Total RNA was isolated from 300 mg of rice roots using an RNeasy plant mini kit (Qiagen) following the manufacturer's instructions. RNA samples were separated by electrophoresis on an agarose gel containing 1.2% formaldehyde and transferred onto a nylon membrane (Amersham). Digoxigenin (DIG)-labeled *PHO1;2* and *cis*-$NAT_{PHO1.2}$ antisense RNA probes were prepared using a DIG RNA labeling kit (Roche). Hybridization was performed under high stringency according to the DIG Nucleic Acid Detection protocol. After washes, filters were exposed and quantified by a phosphor imager (GE Healthcare).

Polysome Gradient Preparation

For polyribosome isolation, roots from 30-d-old wild-type and transgenic plants (*Cis*-$NAT_{PHO1.2}$ RNAi and overexpressing lines) were harvested, frozen, and ground to powder in liquid nitrogen. To prepare cytoplasmic extracts, 150 mg of powder was combined with 1.2 mL of chilled polysome buffer (100 mM Tris-HCl, pH 8.4, 50 mM KCl, 25 mM $MgCl_2$, 5 mM EGTA, 18 μM cycloheximide, 15.5 μM chloramphenicol, and 0.5% [v/v] Nonidet P-40). Debris was removed by centrifugation at 16,000*g* for 15 min at 4°C. Aliquots of the resulting supernatant were loaded on 20 to 50% (w/w) continuous Suc gradients and centrifuged at 32,000 rpm for 165 min in a Beckman SW41 rotor at 4°C. After centrifugation, fractions were collected from the bottom to the top of the gradient with continuous monitoring of the absorbance at 254 nm. Six equal fractions were collected after centrifugation. Six fractions (4 mL per fraction) were collected, 4 mL of Trizol reagent (Invitrogen) was added to each, and RNA was extracted following the manufacturer's instructions. A fixed volume of each RNA sample was then reversed transcribed, and the percentage of mRNA in each fraction was calculated as the percentage of the copy number in a specific fraction to the total copies in the combined six fractions.

Protoplast Preparation and Nuclear Fractionation

For protoplast isolation, green tissues from the stem and sheath of 15 to 20 rice seedlings grown hydroponically in full Pi medium were cut into ~0.5-mm strips. The strips were immediately transferred into 0.5 M mannitol, 4 mM MES-potassium hydroxide, pH 5.5, and 20 mM KCl for 10 min in the dark. The strips were then incubated in an enzyme solution (1.5% Cellulase R10, 0.4% Macerozyme R-10, 0.4 M mannitol, 20 mM MES, pH 5.5, 20 mM KCl, 10 mM $CaCl_2$, and 0.1% BSA) for 4 to 5 h in the dark with gentle shaking (60 to 80 rpm). After the enzymatic digestion, an equal volume of washing solution (WS) containing 154 mM NaCl, 125 mM $CaCl_2$, 5 mM KCl, and 2 mM MES at pH 5.7 was added, followed by vigorous shaking by hand for 10 s. Protoplasts were released by filtering through 40-μm nylon meshes into round-bottom tubes with three to five washes of the strips using WS. Pellets were collected by centrifugation at 1500 rpm for 5 min at 4°C with a swinging bucket. After washing once with WS, pellets were resuspended in nuclei isolation buffer solution (0.1 mM spermidine, 10 mM MES-potassium hydroxide, pH 5.5, 2.5 mM EDTA, 10 mM NaCl, 10 mM KCl, 0.2 M Suc, 0.15% Triton X-10, and 2.5 mM DTT) at a concentration of 10^6 cells mL^{-1}. Samples were incubated on ice for 7 min and then passed four times through syringes with a 25G (5/8) gauge needle. The lysate was filtered through a 20-μm filter into a new tube followed by centrifugation at 400*g* for 10 min. The supernatant was used as the cytoplasmic fraction, and the pellet represents the nuclear fraction. RNA was extracted from both the cytoplasmic and nuclear fractions using 1 volume of Trizol reagent (Invitrogen), following the manufacturer's instructions. A fixed volume of each RNA sample was then reverse transcribed, and the preparation was further used as template for mRNA quantification by quantitative RT-PCR, as described above.

RNA Editing Detection by Direct Sequencing

We generated cDNA clones via RT-PCR from RNAs of wild-type and *cis*-$NAT_{PHO1.2}$ RNAi lines. Reverse transcription was carried out from 1 μg of DNaseI-treated total RNA using oligo(dT) and Moloney murine leukemia virus reverse transcriptase (Promega) according to the manufacturer's instructions. The cDNA produced was diluted with four parts of sterile deionized water. The subsequent PCR amplification of the *PHO1;2* region overlapping with *cis*$NAT_{PHO1.2}$ was performed using the oligonucleotide primers listed in Supplemental Table 1 online, designed to span the introns 1 to 4 to prevent the amplification of residual contaminant genomic DNA. The PCR reaction was performed using KOD high-fidelity polymerase (Novagen) and results in a 1205-bp product. DNA fragment was purified using a Zymoclean Gel DNA recovery kit (Zymo Research) and cloned using the pJET cloning system (Fermentas).

Accession Numbers

Sequence data from this article can be found in the Arabidopsis Genome Initiative or GenBank/EMBL databases under the following accession numbers: AK100323, *PHO1;2*; AK071338, *cis*-NAT$_{PHO1;2}$; and AK121590.1, rice ubiquitin gene.

Supplemental Data

The following materials are available in the online version of this article.

Supplemental Figure 1. Determination of the Activity of the Promoter of *PHO1;2* and *cis*-NAT$_{PHO1;2}$ in Plants Grown under Pi-Sufficient and Pi-Deficient Conditions.

Supplemental Figure 2. Assessment of the Pi Deficiency Status in the Transgenic GUS Lines.

Supplemental Figure 3. GUS Expression Pattern in the Roots of Pro*OsPHO1;2-S*:GUS and Pro*cis*-NAT:GUS Transgenic Lines.

Supplemental Figure 4. Histochemical Localization of GUS Activity in the Flower Organs of Rice Plants Transformed with the *cis*-NATPHO1;2 Promoter:*GUS* Vector.

Supplemental Figure 5. *cis*-NAT Associated with the Maize *PHO1* Transcript.

Supplemental Figure 6. Immunoblot Analysis of PHO1;2 Expression in the Wild Type and *pho1;2* Null Mutants.

Supplemental Figure 7. Silencing of *cis*-NATPHO1;2.

Supplemental Figure 8. RT-PCR Analysis of *PHO1;2* Transcripts.

Supplemental Figure 9. RNA Gel Blot Analysis of Transgenic Lines Expressing an RNAi Construct against the *cis*-NAT$_{PHO1.2}$.

Supplemental Figure 10. Analysis of *PHO1.2* and NAT$_{PHO1.2}$ Export from the Nucleus.

Supplemental Table 1. Primers Used in This Work.

ACKNOWLEDGMENTS

We thank Jurek Paszkowski (University of Geneva), Edward Farmer (University of Lausanne), and members of the Poirier laboratory for helpful discussions. This work was funded by grants from the Swiss National Foundation (31003A-138339) and the Sino-Swiss Science and Technology Cooperation Program (IZLCZ3 123946 to Y.P. and 2009DFA32040 to Q.S.).

AUTHOR CONTRIBUTIONS

M.J. and Y.P. designed and performed the experiments, analyzed the results, and wrote the article. D.S. and C.L. performed the experiments. C.R. and Q.S. designed the experiments, analyzed the results, and wrote the article.

Received July 16, 2013; revised September 3, 2013; accepted September 18, 2013; published October 4, 2013.

REFERENCES

Arpat, A.B., Magliano, P., Wege, S., Rouached, H., Stefanovic, A., and Poirier, Y. (2012). Functional expression of PHO1 to the Golgi and *trans*-Golgi network and its role in export of inorganic phosphate. Plant J. **71:** 479–491.

Au, P.C.K., Zhu, Q.-H., Dennis, E.S., and Wang, M.-B. (2011). Long non-coding RNA-mediated mechanisms independent of the RNAi pathway in animals and plants. RNA Biol. **8:** 404–414.

Bass, B.L. (2002). RNA editing by adenosine deaminases that act on RNA. Annu. Rev. Biochem. **71:** 817–846.

Beltran, M., Puig, I., Peña, C., García, J.M., Alvarez, A.B., Peña, R., Bonilla, F., and de Herreros, A.G. (2008). A natural antisense transcript regulates Zeb2/Sip1 gene expression during Snail1-induced epithelial-mesenchymal transition. Genes Dev. **22:** 756–769.

Borsani, O., Zhu, J.H., Verslues, P.E., Sunkar, R., and Zhu, J.K. (2005). Endogenous siRNAs derived from a pair of natural cis-antisense transcripts regulate salt tolerance in *Arabidopsis*. Cell **123:** 1279–1291.

Bumgarner, S.L., Dowell, R.D., Grisafi, P., Gifford, D.K., and Fink, G.R. (2009). Toggle involving cis-interfering noncoding RNAs controls variegated gene expression in yeast. Proc. Natl. Acad. Sci. USA **106:** 18321–18326.

Carrieri, C., et al. (2012). Long non-coding antisense RNA controls Uchl1 translation through an embedded SINEB2 repeat. Nature **491:** 454–457.

Castel, S.E., and Martienssen, R.A. (2013). RNA interference in the nucleus: Roles for small RNAs in transcription, epigenetics and beyond. Nat. Rev. Genet. **14:** 100–112.

Chen, D., Meng, Y., Ma, X., Mao, C., Bai, Y., Cao, J., Gu, H., Wu, P., and Chen, M. (2010). Small RNAs in angiosperms: Sequence characteristics, distribution and generation. Bioinformatics **26:** 1391–1394.

Chen, X. (2010). Small RNAs - Secrets and surprises of the genome. Plant J. **61:** 941–958.

Curtis, M.D., and Grossniklaus, U. (2003). A gateway cloning vector set for high-throughput functional analysis of genes in planta. Plant Physiol. **133:** 462–469.

Ebralidze, A.K., et al. (2008). PU.1 expression is modulated by the balance of functional sense and antisense RNAs regulated by a shared cis-regulatory element. Genes Dev. **22:** 2085–2092.

Faghihi, M.A., Modarresi, F., Khalil, A.M., Wood, D.E., Sahagan, B.G., Morgan, T.E., Finch, C.E., St Laurent, G., III., Kenny, P.J., and Wahlestedt, C. (2008). Expression of a noncoding RNA is elevated in Alzheimer's disease and drives rapid feed-forward regulation of beta-secretase. Nat. Med. **14:** 723–730.

Faghihi, M.A., and Wahlestedt, C. (2009). Regulatory roles of natural antisense transcripts. Nat. Rev. Mol. Cell Biol. **10:** 637–643.

Franco-Zorrilla, J.M., Valli, A., Todesco, M., Mateos, I., Puga, M.I., Rubio-Somoza, I., Leyva, A., Weigel, D., García, J.A., and Paz-Ares, J. (2007). Target mimicry provides a new mechanism for regulation of microRNA activity. Nat. Genet. **39:** 1033–1037.

Gelfand, B., Mead, J., Bruning, A., Apostolopoulos, N., Tadigotla, V., Nagaraj, V., Sengupta, A.M., and Vershon, A.K. (2011). Regulated antisense transcription controls expression of cell-type-specific genes in yeast. Mol. Cell. Biol. **31:** 1701–1709.

Ghildiyal, M., and Zamore, P.D. (2009). Small silencing RNAs: An expanding universe. Nat. Rev. Genet. **10:** 94–108.

Gong, C., and Maquat, L.E. (2011). lncRNAs transactivate STAU1-mediated mRNA decay by duplexing with 3′ UTRs via Alu elements. Nature **470:** 284–288.

Hamburger, D., Rezzonico, E., MacDonald-Comber Petétot, J., Somerville, C., and Poirier, Y. (2002). Identification and characterization of the *Arabidopsis PHO1* gene involved in phosphate loading to the xylem. Plant Cell **14:** 889–902.

Hastings, M.L., Ingle, H.A., Lazar, M.A., and Munroe, S.H. (2000). Regulation of erbα pre-mRNA alternative processing: Role of *cis*-acting sequences and a naturally occuring antisense RNA. J. Biol. Chem. **275:** 11507–11513.

Held, M.A., Penning, B., Brandt, A.S., Kessans, S.A., Yong, W.D., Scofield, S.R., and Carpita, N.C. (2008). Small-interfering RNAs from natural antisense transcripts derived from a cellulose synthase gene modulate cell wall biosynthesis in barley. Proc. Natl. Acad. Sci. USA **105:** 20534–20539.

Heo, J.B., and Sung, S. (2011). Vernalization-mediated epigenetic silencing by a long intronic noncoding RNA. Science **331:** 76–79.

Hoffer, P., Ivashuta, S., Pontes, O., Vitins, A., Pikaard, C., Mroczka, A., Wagner, N., and Voelker, T. (2011). Posttranscriptional gene silencing in nuclei. Proc. Natl. Acad. Sci. USA **108:** 409–414.

Hou, X.L., Wu, P., Jiao, F.C., Jia, Q.J., Chen, H.M., Yu, J., Song, X.W., and Yi, K.K. (2005). Regulation of the expression of *OsIPS1* and *OsIPS2* in rice via systemic and local Pi signalling and hormones. Plant Cell Environ. **28:** 353–364.

Hung, T., et al. (2011). Extensive and coordinated transcription of noncoding RNAs within cell-cycle promoters. Nat. Genet. **43:** 621–629.

Jabnoune, M., Espeout, S., Mieulet, D., Fizames, C., Verdeil, J.-L., Conéjéro, G., Rodríguez-Navarro, A., Sentenac, H., Guiderdoni, E., Abdelly, C., and Véry, A.-A. (2009). Diversity in expression patterns and functional properties in the rice HKT transporter family. Plant Physiol. **150:** 1955–1971.

Karimi, M., Inzé, D., and Depicker, A. (2002). GATEWAY vectors for Agrobacterium-mediated plant transformation. Trends Plant Sci. **7:** 193–195.

Katayama, S., et al; RIKEN Genome Exploration Research Group; Genome Science Group (Genome Network Project Core Group); FANTOM Consortium (2005). Antisense transcription in the mammalian transcriptome. Science **309:** 1564–1566.

Katiyar-Agarwal, S., Morgan, R., Dahlbeck, D., Borsani, O., Villegas, A., Jr., Zhu, J.-K., Staskawicz, B.J., and Jin, H. (2006). A pathogen-inducible endogenous siRNA in plant immunity. Proc. Natl. Acad. Sci. USA **103:** 18002–18007.

Kim, E.-D., and Sung, S. (2012). Long noncoding RNA: Unveiling hidden layer of gene regulatory networks. Trends Plant Sci. **17:** 16–21.

Kiyosawa, H., Yamanaka, I., Osato, N., Kondo, S., and Hayashizaki, Y. (2003). Antisense transcripts with FANTOM2 clone set and their implications for gene regulation. Genome Res. **13** (6B)**:** 1324–1334.

Lapidot, M., and Pilpel, Y. (2006). Genome-wide natural antisense transcription: Coupling its regulation to its different regulatory mechanisms. EMBO Rep. **7:** 1216–1222.

Lavorgna, G., Dahary, D., Lehner, B., Sorek, R., Sanderson, C.M., and Casari, G. (2004). In search of antisense. Trends Biochem. Sci. **29:** 88–94.

Li, J.T., Zhang, Y., Kong, L., Liu, Q.R., and Wei, L.P. (2008). Trans-natural antisense transcripts including noncoding RNAs in 10 species: Implications for expression regulation. Nucleic Acids Res. **36:** 4833–4844.

Li, L., Wang, X.F., Stolc, V., Li, X.Y., Zhang, D.F., Su, N., Tongprasit, W., Li, S.G., Cheng, Z.K., Wang, J., and Deng, X.W. (2006). Genome-wide transcription analyses in rice using tiling microarrays. Nat. Genet. **38:** 124–129.

Lin, S.I., Chiang, S.F., Lin, W.Y., Chen, J.W., Tseng, C.Y., Wu, P.C., and Chiou, T.J. (2008). Regulatory network of microRNA399 and PHO2 by systemic signaling. Plant Physiol. **147:** 732–746.

Liu, F., Marquardt, S., Lister, C., Swiezewski, S., and Dean, C. (2010). Targeted 3′ processing of antisense transcripts triggers *Arabidopsis* FLC chromatin silencing. Science **327:** 94–97.

Liu, T.-Y., Huang, T.-K., Tseng, C.-Y., Lai, Y.-S., Lin, S.-I., Lin, W.-Y., Chen, J.-W., and Chiou, T.-J. (2012). PHO2-dependent degradation of PHO1 modulates phosphate homeostasis in *Arabidopsis*. Plant Cell **24:** 2168–2183.

Martianov, I., Ramadass, A., Serra Barros, A., Chow, N., and Akoulitchev, A. (2007). Repression of the human dihydrofolate reductase gene by a non-coding interfering transcript. Nature **445:** 666–670.

Meng, Y.J., Chen, D., Jin, Y.F., Mao, C., Wu, P., and Chen, M. (2010). RNA editing of nuclear transcripts in *Arabidopsis thaliana*. BMC Genomics **11** (suppl. 4)**:** S12.

Miki, D., and Shimamoto, K. (2004). Simple RNAi vectors for stable and transient suppression of gene function in rice. Plant Cell Physiol. **45:** 490–495.

Misra, S., et al. (2002). Annotation of the *Drosophila melanogaster* euchromatic genome: A systematic review. Genome Biol. **3:** H0083.

Misson, J., et al. (2005). A genome-wide transcriptional analysis using *Arabidopsis thaliana* Affymetrix gene chips determined plant responses to phosphate deprivation. Proc. Natl. Acad. Sci. USA **102:** 11934–11939.

Morcuende, R., Bari, R.P., Gibon, Y., Zheng, W., Pant, B.D., Bläsing, O., Usadel, B., Czechowski, T., Udvardi, M.K., Stitt, M., and Scheible, W.R. (2007). Genome-wide reprogramming of metabolism and regulatory networks of *Arabidopsis* in response to phosphorus. Plant Cell Environ. **30:** 85–112.

Müller, R., Morant, M., Jarmer, H., Nilsson, L., and Nielsen, T.H. (2007). Genome-wide analysis of the Arabidopsis leaf transcriptome reveals interaction of phosphate and sugar metabolism. Plant Physiol. **143:** 156–171.

Okamura, K., Balla, S., Martin, R., Liu, N., and Lai, E.C. (2008). Two distinct mechanisms generate endogenous siRNAs from bidirectional transcription in *Drosophila melanogaster*. Nat. Struct. Mol. Biol. **15:** 581–590.

Ørom, U.A., Derrien, T., Beringer, M., Gumireddy, K., Gardini, A., Bussotti, G., Lai, F., Zytnicki, M., Notredame, C., Huang, Q., Guigo, R., and Shiekhattar, R. (2010). Long noncoding RNAs with enhancer-like function in human cells. Cell **143:** 46–58.

Osato, N., et al. (2003). Antisense transcripts with rice full-length cDNAs. Genome Biol. **5:** R5.

Pant, B.D., Musialak-Lange, M., Nuc, P., May, P., Buhtz, A., Kehr, J., Walther, D., and Scheible, W.R. (2009). Identification of nutrient-responsive Arabidopsis and rapeseed microRNAs by comprehensive real-time polymerase chain reaction profiling and small RNA sequencing. Plant Physiol. **150:** 1541–1555.

Ponting, C.P., Oliver, P.L., and Reik, W. (2009). Evolution and functions of long noncoding RNAs. Cell **136:** 629–641.

Rinn, J.L., and Chang, H.Y. (2012). Genome regulation by long noncoding RNAs. Annu. Rev. Biochem. **81:** 145–166.

Rinn, J.L., Kertesz, M., Wang, J.K., Squazzo, S.L., Xu, X., Brugmann, S.A., Goodnough, L.H., Helms, J.A., Farnham, P.J., Segal, E., and Chang, H.Y. (2007). Functional demarcation of active and silent chromatin domains in human HOX loci by noncoding RNAs. Cell **129:** 1311–1323.

Ron, M., Alandete Saez, M., Eshed Williams, L., Fletcher, J.C., and McCormick, S. (2010). Proper regulation of a sperm-specific cis-nat-siRNA is essential for double fertilization in *Arabidopsis*. Genes Dev. **24:** 1010–1021.

Rouached, H., Stefanovic, A., Secco, D., Bulak Arpat, A., Gout, E., Bligny, R., and Poirier, Y. (2011). Uncoupling phosphate deficiency from its major effects on growth and transcriptome via PHO1 expression in *Arabidopsis*. Plant J. **65:** 557–570.

Rubio, V., Linhares, F., Solano, R., Martín, A.C., Iglesias, J., Leyva, A., and Paz-Ares, J. (2001). A conserved MYB transcription factor involved in phosphate starvation signaling both in vascular plants and in unicellular algae. Genes Dev. **15:** 2122–2133.

Secco, D., Baumann, A., and Poirier, Y. (2010). Characterization of the rice PHO1 gene family reveals a key role for OsPHO1;2 in phosphate homeostasis and the evolution of a distinct clade in dicotyledons. Plant Physiol. **152:** 1693–1704.

Simon, A.E., and Miller, W.A. (2013). 3′ Cap-independent translation enhancers of plant viruses. Annu. Rev. Microbiol. **67:** 21–42.

Stefanovic, A., Arpat, A.B., Bligny, R., Gout, E., Vidoudez, C., Bensimon, M., and Poirier, Y. (2011). Over-expression of PHO1 in *Arabidopsis* leaves reveals its role in mediating phosphate efflux. Plant J. **66:** 689–699.

Stefanovic, A., Ribot, C., Rouached, H., Wang, Y., Chong, J., Belbahri, L., Delessert, S., and Poirier, Y. (2007). Members of the *PHO1* gene family show limited functional redundancy in phosphate transfer to the shoot, and are regulated by phosphate deficiency via distinct pathways. Plant J. **50:** 982–994.

Swiezewski, S., Crevillen, P., Liu, F., Ecker, J.R., Jerzmanowski, A., and Dean, C. (2007). Small RNA-mediated chromatin silencing directed to the 3′ region of the Arabidopsis gene encoding the developmental regulator, FLC. Proc. Natl. Acad. Sci. USA **104:** 3633–3638.

Swiezewski, S., Liu, F., Magusin, A., and Dean, C. (2009). Cold-induced silencing by long antisense transcripts of an *Arabidopsis* Polycomb target. Nature **462:** 799–802.

Uchimiya, H., Iwata, M., Nojiri, C., Samarajeewa, P.K., Takamatsu, S., Ooba, S., Anzai, H., Christensen, A.H., Quail, P.H., and Toki, S. (1993). Bialaphos treatment of transgenic rice plants expressing a *bar* gene prevents infection by the sheath blight pathogen (*Rhizoctonia solani*). Nature Biotechnol. **11:** 835–836.

Wang, H., Chua, N.-H., and Wang, X.-J. (2006). Prediction of trans-antisense transcripts in *Arabidopsis thaliana*. Genome Biol. **7:** R92.

Wang, K.C., et al. (2011). A long noncoding RNA maintains active chromatin to coordinate homeotic gene expression. Nature **472:** 120–124.

Wang, X.J., Gaasterland, T., and Chua, N.H. (2005). Genome-wide prediction and identification of cis-natural antisense transcripts in *Arabidopsis thaliana*. Genome Biol. **6:** R30.

Watanabe, T., et al. (2008). Endogenous siRNAs from naturally formed dsRNAs regulate transcripts in mouse oocytes. Nature **453:** 539–543.

Woo, J., MacPherson, C.R., Liu, J., Wang, H., Kiba, T., Hannah, M.A., Wang, X.-J., Bajic, V.B., and Chua, N.-H. (2012). The response and recovery of the *Arabidopsis thaliana* transcriptome to phosphate starvation. BMC Plant Biol. **12:** 62.

Yan, M.D., Hong, C.C., Lai, G.M., Cheng, A.L., Lin, Y.W., and Chuang, S.E. (2005). Identification and characterization of a novel gene Saf transcribed from the opposite strand of Fas. Hum. Mol. Genet. **14:** 1465–1474.

Yelin, R., et al. (2003). Widespread occurrence of antisense transcription in the human genome. Nat. Biotechnol. **21:** 379–386.

Young, H.A., Subleski, J.J., and Krebs, S.M. (2003). Multiprobe ribonuclease protection assay for simultaneous measurement of mRNA expression. Curr. Protoc. Immunol. **54:** 10.29.1–10.29.15.

Zhang, X., et al. (2012). Genome-wide analysis of plant nat-siRNAs reveals insights into their distribution, biogenesis and function. Genome Biol. **13:** R20.

Zhang, Y., Liu, X.S., Liu, Q.-R., and Wei, L. (2006). Genome-wide in silico identification and analysis of cis natural antisense transcripts (cis-NATs) in ten species. Nucleic Acids Res. **34:** 3465–3475.

Zhao, J., Sun, B.K., Erwin, J.A., Song, J.-J., and Lee, J.T. (2008). Polycomb proteins targeted by a short repeat RNA to the mouse X chromosome. Science **322:** 750–756.

Zhou, X.F., Sunkar, R., Jin, H.L., Zhu, J.K., and Zhang, W.X. (2009). Genome-wide identification and analysis of small RNAs originated from natural antisense transcripts in *Oryza sativa*. Genome Res. **19:** 70–78.

Zubko, E., and Meyer, P. (2007). A natural antisense transcript of the *Petunia hybrida* Sho gene suggests a role for an antisense mechanism in cytokinin regulation. Plant J. **52:** 1131–1139.